

We thank the two reviewers for their efforts and for the feedback that helped to improve the manuscript. A point-by-point response to all comments is given below (referee comments are highlighted in red). We have considered all comments made and a revised manuscript is submitted along this response. Figure and line numbers refer to the revised manuscript unless otherwise noted. Figures only appearing in this document are labelled with Roman numbers (e.g. I, II, III, ...).

Sect. 3.2 *Detecting surface coupling* was extended to make the methodology and the reasoning behind it more understandable. Specifically, Fig. 2a in the original manuscript was replaced with two example cases. Following this the order of appearance of Figures 2 and 3 changed, so that Fig. 2 and 3 have swapped places in the revised manuscript. While the manuscript was in review, some additional microwave radiometer data become available and has been included in the analysis leading to a slight change in some values but not altering any of the conclusions of the paper. As advised by Referee #2, Sect. 2.3 *Circulation weather type* was moved under Sect. 3. In Sect. 3.4 *Local wind conditions* a paragraph was added to give more information on the local wind climate at the site based on the existing literature, and the description on the wind conditions based on sounding profiles was shortened. This also lead to excluding Fig. 5b and merging Fig. 5a with Fig. 4.

As suggested by Referee #2, the Results and Discussion (titled *A consolidated view of P-MPC at Ny-Ålesund* in the original manuscript) sections have been restructured so that the discussion is placed together with the presentation of the corresponding results. Sect. 4 is now titled “*Results and discussion*” with thematic subsections. Following the comments from both reviewers, a section on seasonality has been added, and the figure on the seasonality of cloud base height (Fig. 11c in the original manuscript) was moved from the section on coupling to this section. The section *Local wind patterns around Ny-Ålesund* has been moved to the end of the *Results and discussion* -section. The Results and discussion -section therefore now consists of five subsections: 4.1 *Occurrence of persistent MPC and other clouds*, 4.2 *P-MPC properties and regional wind direction*, 4.3 *Seasonality*, 4.4 *Surface coupling* and 4.5 *Local wind patterns around Ny-Ålesund*. The results regarding the connection of coupling and local winds have been moved from Sect. 4.4 to Sect. 4.5. Furthermore, the detailed results on the influences of local winds on cloud properties given in Sect. 4.5 *Local wind patterns around Ny-Ålesund* have been moved to the Appendix. Moreover, distributions of integrated water vapour and atmospheric temperature have been added in Sect. 4.2 following the comments from Referee #1.

The newly added Appendix A *Details on the relationship between local wind conditions and P-MPC* has two parts: A1 consists of the results and related discussion moved from Sect. 4.5.. Sect. A2 *Seasonality of surface wind direction and P-MPC coupling* presents additional seasonal figures for surface wind and occurrence of cloud coupling with different surface wind direction classes (same figures as Fig. 4a and 11b of the revised manuscript, respectively, but for each season).

A document detailing the changes made in the manuscript created by latexdiff is provided at the end of this document. In order to clearly communicate the changes in content, we first reorganised the text before running latexdiff. Hence, a block of text that was moved from one section to another does not appear as new text marked with blue.

Reply to Referee #1

(1) Moisture

This study describes three items, namely, properties of persistent MPC (P-MPC), local wind directions (surface and 850 hPa), and coupling/decoupling between the cloud layer and surface. Key parameters that connect these three items are temperature and moisture. Although some plots are shown for cloud top temperature, no data is presented for moisture. The authors may show integrated water vapor (IWV) obtained by MWR and atmospheric temperature to describe relationships among the three items.

For example, under the westerly conditions at 850 hPa (from open ocean), did the authors observe higher IWV and temperature as compared with those under easterly conditions (from island)? Did they observe higher IWV for coupled clouds as compared with those for decoupled clouds?

We thank the referee for this comment. While some description of the climatology of atmospheric moisture and temperature in the atmospheric column above Ny-Ålesund and the dependence on air mass origin is available in the literature (e.g. Dahlke and Maturilli, 2017), we agree that these important parameters ought to be described more in detail, especially in the context of the persistent mixed-phase clouds (P-MPC) that are the topic of this paper. As pointed out by the referee, this data is available from the micro-wave radiometer (MWR). We evaluated the distributions of integrated water vapour (IWV) and temperature at 1.5 km (corresponding to a typical height of the 850 hPa level) retrieved from the MWR, including only the time periods when P-MPCs were identified above Ny-Ålesund. The dependency of these parameters on regional wind direction (e.g. the weather type used in our study) and season have been included in Sections 4.2 and 4.3, respectively. To which extent the variations in atmospheric humidity and temperature can explain the observed variations in P-MPC occurrence and properties are shortly discussed in the corresponding sections.

To respond to the question on the relationship between P-MPC coupling and IWV, we have included Fig. I showing the IWV distributions for coupled, predominantly decoupled and fully decoupled P-MPC. Similarly to the cloud top temperatures presented (Fig. 12c), the coupled and predominantly decoupled occurred in rather similar humidity conditions, while the fully decoupled are associated with slightly drier atmospheric conditions. This is in agreement with the other results showing that the fully decoupled P-MPC have lower cloud top temperature, and occur most often in winter when IWV is lower. Analogous to the cloud top temperature, the IWV distributions are not able to explain the similarity of the IWP and LWP distributions of fully and predominantly decoupled P-MPC, or the differences between the coupled and predominantly decoupled P-MPC.

Changes in the manuscript:

- Figure 8 was added to show the atmospheric humidity and temperature connections associated with the P-MPC and different weather types. The following text was added:

“Here we use temperature at 1.5 km (corresponding to the 850~hPa level) and integrated water vapor (IWV) from the MWR to represent the atmospheric temperature and humidity conditions under which the P-MPC were occurring. In agreement with previous studies, Fig. 8 shows that the highest average IWV and warmest temperatures were associated with southerly winds, while the lowest

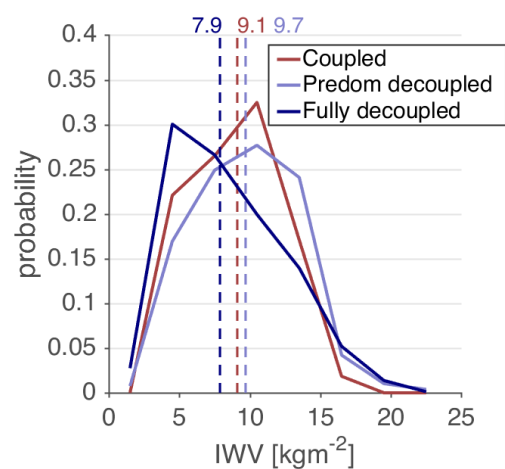


Figure I. Distributions of IWV for coupled, predominantly decoupled and fully decoupled P-MPC. The dashed line and the numbers on top show the median value of each distribution. The bin size is 3 kgm⁻². The medians were found to differ on a 95 % confidence level.

average IWV and coldest temperatures with northerly winds. The domain considered for the weather type (Fig. 1a) is too small to describe large scale advection or air mass origin, but Fig. 8 suggests the weather type is nonetheless a useful proxy for air mass properties. The average IWV and 1.5 km temperature can explain the first order variation in P-MPC occurrence and LWP between weather types. The south-southwesterly winds are warm and humid, and are associated with frequent occurrence of P-MPC with relatively high amounts of liquid, compared to the north-northeasterly winds, which are drier and colder, and are associated with less frequent P-MPC occurrence and lower LWP (Fig. 6, 7b, and 8a). Owing to the complexity of ice micro-physical processes, such direct relationship cannot be found between atmospheric humidity and temperature (Fig. 8) and IWP (Fig. 7c). On the other hand, as already noted above, Fig. 8 shows a clear contrast between the properties of easterly and westerly P-MPC. These differences cannot be explained by the IWV and 1.5 km temperature distributions, which are rather similar for weather types W and E. Hence, atmospheric temperature and humidity are important, but not the only relevant forcing for P-MPC at Ny-Ålesund.” (L. 355-368)

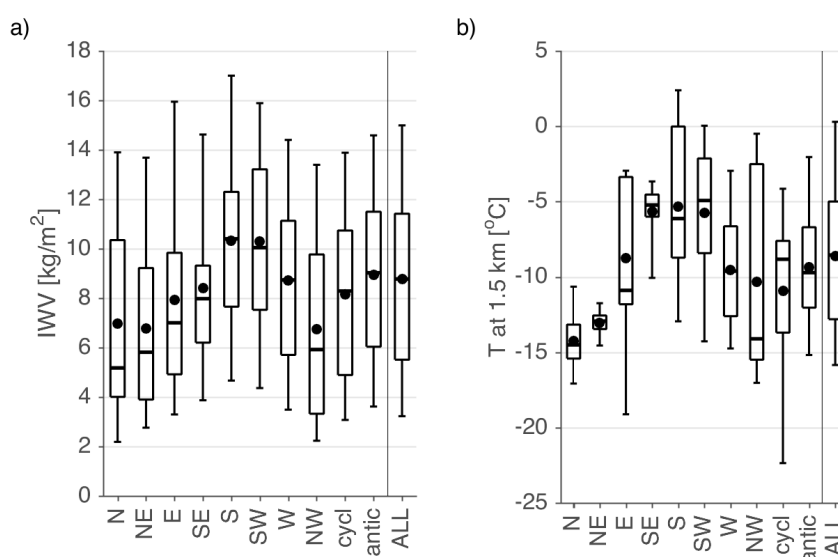


Figure 8. IWV (a) and 1.5 km temperature (b) for time periods with P-MPC present for each weather type. The box shows the 25th, 50th and 75th percentile, the dot the mean, and the whiskers indicate the 5th and 95th percentile. The medians were found to differ on a 95 % confidence level.

- The Sect 4.2 is now summarized in the last paragraph as follows:

“The combination of the effects of large scale advection and air mass properties, as well as the influence of the Svalbard archipelago, can provide an explanation for the dependence of the P-MPC properties on weather type presented in Fig. 6 and 7. Southwesterly and westerly free-tropospheric winds were associated with most P-MPC and the highest average LWP and IWP, likely due to higher amounts of humidity available from lower latitudes. The southeasterly to northeasterly winds had the least P-MPC, and comprise the lowest average LWP and IWP, related to the drier air masses from north and less favourable conditions for cloud formation over the island. Other mechanisms can be considered to further explain the observed IWP variation. Ice formation could be enhanced in the cold temperatures for weather types N and NE (Fig. 8), whereas the higher IWP for weather types SW, W and NW might be related to larger amounts of super-cooled liquid available in the P-MPCs (Fig. 7b,c) or higher aerosol concentration in airmasses advected from lower latitudes.” (L. 380-388)

- The source of the IWV was added in Sect. 2.2.3 (new text in bold):

“In addition, humidity supply is a key requirement for cloud formation and continuation. Liquid water path (LWP) and integrated water vapor (I WV) were retrieved from [...]” (L. 135-137)

(2) Seasonality

In most of analyses, all data were used irrespective of month when the data was obtained. However, the authors may show the results from viewpoint of seasonality.

For example the authors may show seasonal variations of liquid layer base height, LWP, and IWP. (If they can also show cloud thickness and time duration of clouds (cloud persistence), it would be nice).

The authors may also show wind rose at 850 hPa in four seasons to show how the higher LWP under the westerly conditions at 850 hPa (Fig. 8b) reflects the seasonal variations in wind direction.

We understand this comment to consists of three main points, namely: 1) a suggestion to consider the seasonality of the presented properties, and to show the seasonal variation of cloud base height, LWP and IWP, 2) a proposal to also consider the seasonal variation of additional cloud properties, i.e. geometrical thickness and duration of the P-MPC, and 3) the advice to demonstrate how the seasonality in 850 hPa wind direction is related to the relationship between LWP and wind direction presented in Sect 4.2. We respond to these three remarks one by one.

The manuscript only considered the seasonality of cloud occurrence and surface coupling of P-MPC. Additionally, the seasonal variation of cloud base height was shown because this was relevant to correctly interpret the variation of cloud base height of coupled and decoupled clouds, as coupling was found to be seasonally dependent. As noted by the referee, seasonal variation of P-MPC properties in themselves were not thematized. To correct for this shortcoming, we have added a section (Sect. 4.3) describing the seasonality of P-MPC properties, as well as atmospheric humidity and moisture due to their role as key air mass properties related to the P-MPCs. We have moved relevant parts of the originally submitted manuscript to this section (specifically: the seasonal variation of cloud base height, comparison with results from other sites as well as previous studies from Svalbard region), as well as added a description of the seasonality of LWP, IWP, IWV and 1.5 km temperature (Fig 9, L. 390-415).

For the second aspect, considering the seasonal variation of P-MPC geometrical thickness and duration, these variables are presented in Fig. II. The depth of the P-MPC, defined here as the distance from liquid cloud base to cloud top (the last bin detected by either radar or ceilometer), did not show notable seasonal variation. The mean P-MPC depth varied from 360 to 390 m. Due to the lack of seasonality we don't find this result interesting enough to include in the manuscript. Secondly, the duration of each P-MPC case (L. 172-173: “A P-MPC case was defined as the time from the beginning to the end of the identified persistent liquid layer.”) shows seasonal variation. On average, the cases are shorter in winter and longer in duration in summer. However, individual very persistent cases are found in all seasons, and the longest persisting case (63 h) occurred in winter. Since our P-MPC identification algorithm is heavily relying on the persistence of a liquid layer, the thresholds set in the algorithm have a direct influence on the P-MPC duration. Let us consider an example cloud that has a liquid layer persisting for 3 h with a 4 min gap half way. If we only allow gaps up to 3 min this cloud would be considered as 2 cases with a duration of 1 h 28 min each. If instead a 5 min gap is allowed, only one case with a duration of 3 h is identified. This example illustrates how cloud persistence is build in our P-MPC detection algorithm. Although we found a similar seasonal cycle in our sensitivity tests for the persistence criteria, we are cautious to present quantitative results on P-MPC duration and this result was not included in the revised manuscript.

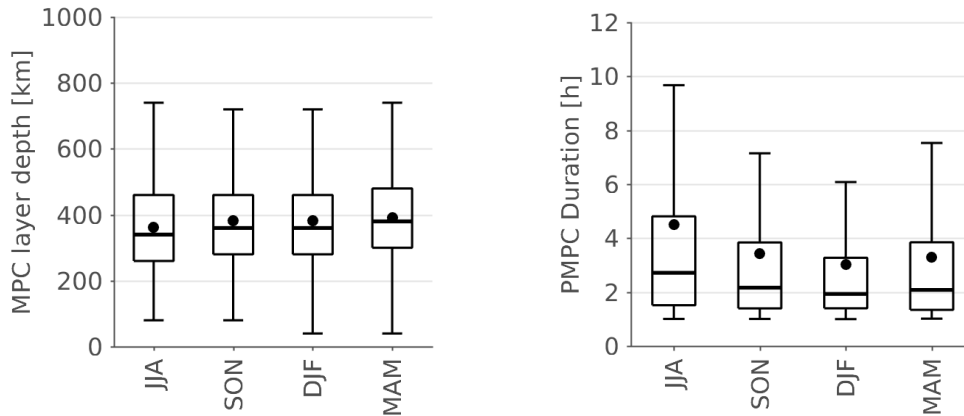


Figure II. Seasonal variation of P-MPC thickness (left) and duration (right).

Lastly, the referee pointed out that it would be worth to consider the seasonal variation in the 850 hPa wind direction, and whether this could explain some of the relationships between wind direction and P-MPC properties (specifically LWP) identified in Sect. 4.2. We have considered this possibility and found no seasonal variation in the weather type (used to describe the regional wind field at 850 hPa) that could explain the observed differences in cloud occurrence and properties between different weather types. To allow others to make the same conclusion, we have added a figure presenting the seasonal occurrence of all weather types (Fig. 10) in the manuscript.

Changes in the manuscript:

Section 4.3 *Seasonality* (L. 389-450) was added to describe the seasonal variability of key parameters. To avoid copying the entire section here, we only summarize the content of the section and provide the figures and new results here. For complete Sect. 4.3 we kindly ask to consult the attached manuscript.

- Sect. 4.3 includes the description of seasonality of the cloud base height, which was previously presented together with P-MPC coupling and the relationship between coupling and cloud base height (L. 392-393). In addition, Fig. 9 includes the seasonal variation of IWV, 1.5 km temperature, LWP and IWP, together with the following texts:

“The seasonal variation of the studied P-MPC properties and atmospheric conditions at Ny-Ålesund are presented in Fig. 9. In agreement with previous studies (Nomokonova et al., 2019b; Maturilli and Kayser, 2017), the highest average temperature and humidity are found in summer, and the lowest in winter and spring (Fig. 9a,b).” (L. 390-392)

“The IWP distributions show a clear seasonality, with low values in summer and autumn and a clear maxima in spring (Fig. 9e). The low IWP in summer and autumn (median 0.2 and 1.0 gm^{-2} , respectively) can be attributed to relatively warm temperatures close to 0°C . The median IWP in spring (7.5 gm^{-2}) is almost 2-fold of the median IWP in the winter (4.0 gm^{-2}), which can hardly be attributed to the different temperature conditions (Fig. 9b). The higher IWV in spring compared to winter (Fig. 9a), however, can play a role. Furthermore, the high IWP in spring could be related to the generally higher aerosol loading in the Arctic atmosphere in the late winter and spring, a time period also known as the Arctic haze season (Quinn et al., 2007).

On the contrary, the LWP distributions show a minimal seasonality despite the seasonal variation of IWV and 1.5 km temperature related to the P-MPC (Fig. 9a,b,d). The highest (lowest) median LWP in summer and spring (winter) was 24 gm^{-2} (18 gm^{-2}), and the seasonal mean values varied from 33

to 36 gm^{-2} . Note, that this result does not imply a lack of seasonal variability in overall cloud LWP (see Fig. 5 in Nomokonova et al., 2019a), only in the specific cloud regime evaluated.” (L. 396-406)

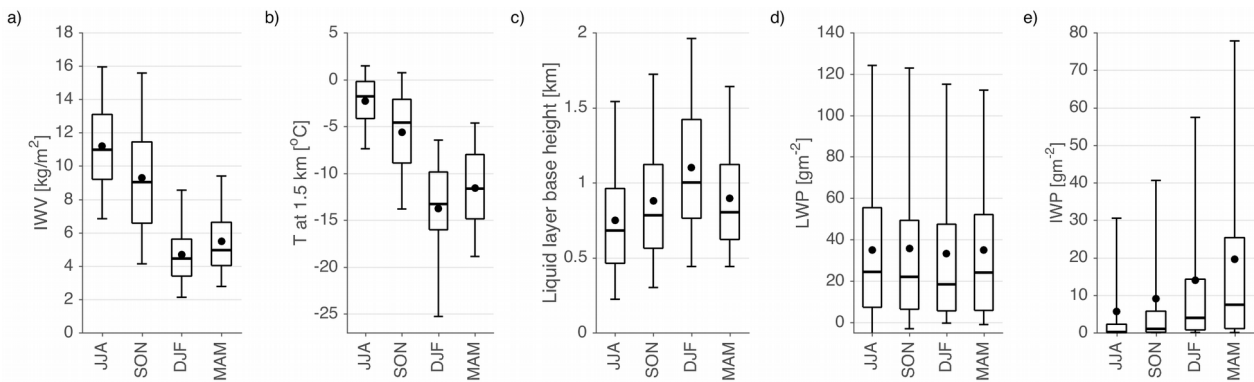


Figure 9. IWV (a), 1.5 km temperature (b), liquid base height (c), LWP (d) and IWP (e) distributions for each season. Only time periods with P-MPCs present are included. Boxes and whiskers as in Fig. 7; the medians were found to differ on a 95 % confident level.

- The consideration of the P-MPC detection algorithms limitation regarding to thick liquid layers was moved to this section from 4.2 P-MPC properties and regional wind direction, and a sentence commenting on the possibility of the cloud identified cloud regime leading to the lack of seasonality in LWP was added:

“In addition, it could be that the cloud detection algorithm limits the considered cases to a specific LWP regime, which results to the lack of seasonality in the LWP of the P-MPC.” (L.412-414)

- To clearly demonstrate that the dependency of P-MPC on weather types presented in Sect. 4.2 is not a result in seasonal variation of P-MPC occurrence and properties combined with a seasonality in 850 hPa wind direction, Fig. 10 is included with the following text:

“Since P-MPC properties (excluding LWP) as well as atmospheric temperature and humidity vary seasonally, a seasonal dependency in wind direction could explain the weather type dependent variations in P-MPC properties found in Sect. 4.2. To examine this possibility, Fig. 10 shows the proportion of P-MPC observations in each season for every weather type. The observation period of 2.5 years from June 2016 to October 2018 together with the seasonal variation in P-MPC occurrence (Fig. 5) lead to the uneven distribution of data between seasons. Overall, the summer months contribute most to the data set. However, there are no extensive differences found between the weather types. Most noteworthy is the high spring and low autumn occurrence of NW, which might contribute to the high IWP for this weather type (Fig. 7c). Furthermore, N and E were relatively more common in winter, N and SE more common in spring, and N less common in autumn. Given

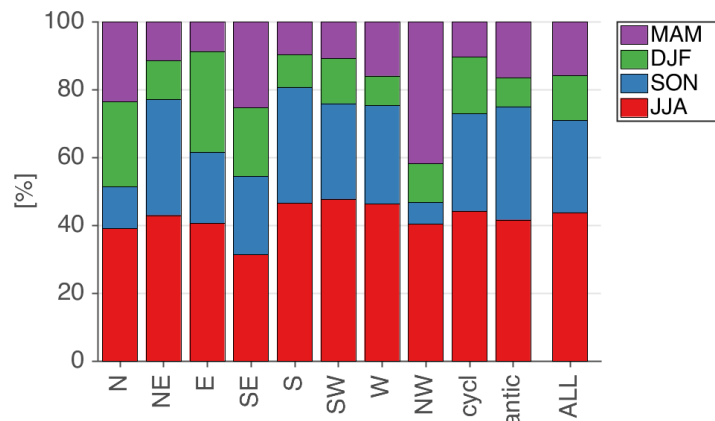


Figure 10. Distribution of seasons in the studied data set for each weather type. Only time periods when a P-MPC was present are included to evaluate the possible impact of wind direction seasonality on cloud properties and occurrence.

the observation period of 2.5 years from June 2016 to October 2018 together with the seasonal variation in P-MPC occurrence (Fig. 5) lead to the uneven distribution of data between seasons. Overall, the summer months contribute most to the data set. However, there are no extensive differences found between the weather types. Most noteworthy is the high spring and low autumn occurrence of NW, which might contribute to the high IWP for this weather type (Fig. 7c). Furthermore, N and E were relatively more common in winter, N and SE more common in spring, and N less common in autumn. Given

the lack of clear trends, we believe the seasonal variation in wind direction plays a minor role in the weather type dependent differences in P-MPC occurrence and properties described in the previous section.” (L. 416-425)

- The comparison of the results with those from other sites and previous studies in the Svalbard area were included in this section (L. 515-537 in the original manuscript), and extended to consider seasonality.

- In the Abstract the following sentence was added:

“Seasonal variation of the liquid water path was found to be minimal, although the occurrence of persistent MPCs, their height and ice water path all showed notable seasonal dependency.” (L. 11-12)

- In Sect. 5 *Conclusions* the following was added:

“P-MPC were found to be higher in winter and lower in summer. LWP presented a lack of seasonal variation, possibly due to the selection of the cloud regime in this study. On the other hand, IWP had a clear seasonal dependence. IWP was low in the relatively warm months of summer and autumn, and had a clear maxima in spring” (L.574-577)

L.135: Explain what is “Ze”.

Ze is defined when first mentioned in Section 2.2.2, on p. 5 L. 127.

L.135-137: The accuracy in LWP is described as 20-25 g m⁻². Uncertainties in IWP is described to be -33 to +50 %. Most of the differences in LWP and IWP for different wind directions presented in this study appeared to be within these uncertainties. What are the precision (uncertainties in relative values) in LWP and IWP estimations? Are the results presented in this study statistically significant?

A relatively high level of uncertainty is an unfortunate aspect of the retrievals available. We compared all distributions presented following the methods described in Sect. 3.5 *Statistical tools*, and all figure captions include the information which medians were found to differ on a statistically significant level. All results described in the text are statistically significant, unless described as “not significant”, for example “The median LWP did not differ significantly between the predominantly and fully decoupled P-MPC” (L. 465-466) and “The medians did not vary significantly” (L. 468). The word *significant* is reserved to only describe statistical significance. We have now double checked the use of the word in the manuscript, and the one omission to this practice has been corrected.

Changes in the manuscript:

L. 313: significant → notable

L.194: What is the basis for this criteria? The authors may show some statistical results for vertical profiles of potential temperature in an appendix to show these criteria are reasonable.

Are all data with positive gradient in potential temperature discarded? No threshold value?

The referee is questioning the basis of the criteria for the stability of the surface layer, namely using the gradient of the 30 min mean potential temperature between 2 and 10 m. Using the potential temperature profile for estimating stratification in the surface layer does not differ from the principle from using the potential temperature profile for the entire subcloud layer. A positive gradient is used in both cases as an indicator for a stable stratified layer. The threshold value is explicitly zero, above this value the layer is considered stable stratified (and with that the cloud decoupled from the surface). As a time series is available from the surface measurements, a 30 min mean was used to ignore the impact of small scale fluctuation caused by individual eddies. This averaging period is common for micro-meteorological studies in the boundary layer (Stull, 1988, p. 33). No data is discarded based on the surface layer stability criteria, only a classification for a decoupled cloud is made. If the cloud is not found decoupled based on the surface layer stability criteria, the second criteria based on MWR is used.

To reply to the question if the criteria whether the potential temperature gradient ($\Delta\theta$) is reasonable, we compared it with the the bulk-Richardson number (Ri_B)

$$Ri_B = \frac{g \Delta\theta \Delta z}{\theta (\Delta U)^2} \quad (1)$$

for the 2 to 10 m layer using the surface meteorological data (Stull, 1988, p. 177). The Richardson number describes the ratio of buoyant and mechanical production of turbulent kinetic energy. A critical value Ri_{crit} of 0.25 is used to define stable stratification. The relationship between the temperature gradient and Ri_B is presented in Fig. III. The two approaches for determining surface layer stability agree 72 % of the time. Disagreement occurs when $\Delta\theta$ is positive, but Ri_B indicates a turbulent layer due to high wind shear. Considering also the limitations related to Ri_B , we think the use of $\Delta\theta$ is justified. Furthermore, using $\Delta\theta$ in the surface layer is consistent with the second criteria used for coupling, which is based on $\Delta\theta$ for a deeper layer using the temperature profiles from the MWR measurements.

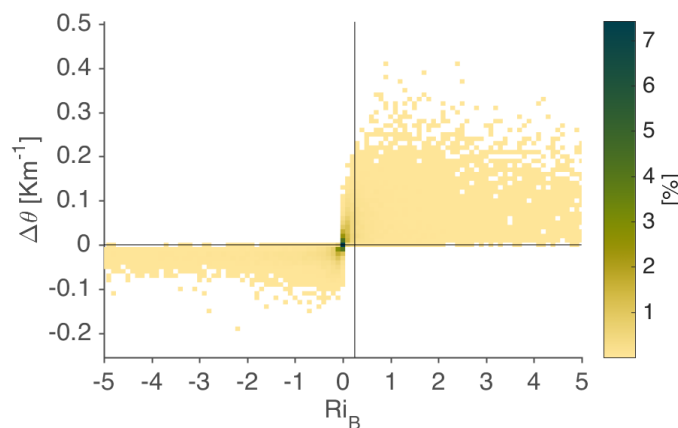


Figure III. Relationship between bulk Richardson number and potential temperature gradient.

Changes to the manuscript

The description of the coupling detection method (Sect 3.2) has been extended to better explain the method and the reasoning behind it.

- To better explain the use of the surface observations, the following text was added (new text is in bold):

“The premise of this criteria is that if the surface layer is stably stratified, the cloud must be decoupled from the surface as there exists a stable layer between the surface and cloud base. The θ -profile is used as a proxy for stability. If the gradient of the 30 min mean θ between 2 and 10 m was positive (e.g. an inversion was present between 2 and 10 m)“

Figure 3: This figure is difficult to see. The authors may expand the figure to show the altitude range between 0 and 2 km and time period between 03:00-12:00.

We thank the referee for the feedback. We increased figure size and limited to the height and time period presented somewhat with the aim to increase the quality of the figure. However, we want to include also the cloud system present until 29 May 2018 01 UTC to make clear that there are clouds clearly identifiable as mixed-phase that were not included in our study.

Changes in the manuscript:

Modification of the Fig 2 (Fig 3 in the original manuscript) to increase figure clarity.

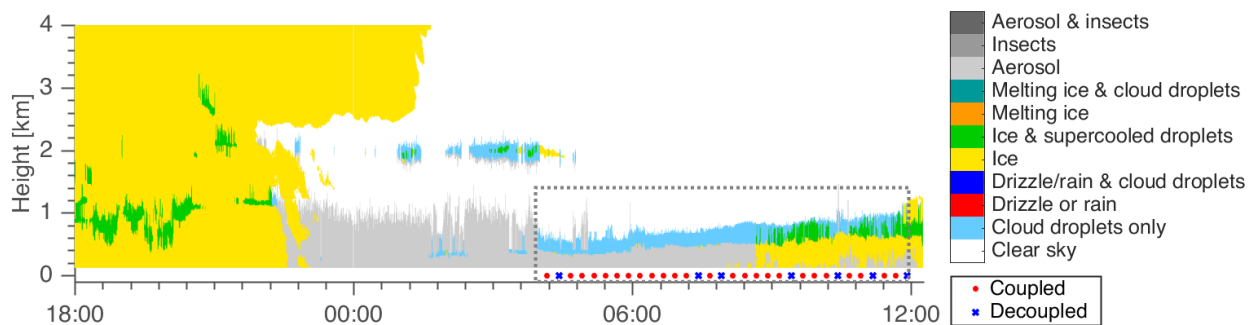


Figure 2. Example of the Cloudnet target classification product from 29 May, 18 UTC to 30 May 2018, 12 UTC. For the P-MPC, indicated by the gray dashed box, also the time series of coupling is shown. This case was classified as coupled.

L.315 (Fig.8a): The authors may compare the cloud base height with lifting condensation level (LCL) calculated from surface measurements.

Figure IV shows the lifting condensation level (LCL) calculated from the surface meteorological observations for all times when P-MPC were present and for each weather type (analogous to Fig. 8a in the original manuscript), as well as a comparison with the LCL and the cloud base height. The LCL was on average below 500 m, which is clearly lower the median cloud base height, which for P-MPC was 760 m (Sect. 4.2, L. 340). Similarly to cloud base height, the LCL was lower for westerly free tropospheric winds and higher for winds from N to SE. Comparing LCL to the cloud base (negative values indicate LCL below cloud base) underlines that cloud base height was usually above the LCL. There seems to be a dependency with wind direction, such that the P-MPC that were on average highest (weather types NE-SE, see Fig. 7a) are also the furthest away of the LCL. The P-MPC that were on average lowest (weather types SW-NW) were also closer to the LCL. This implies that the near surface air is further from condensation, either warmer or drier, for the easterly wind directions than westerly wind directions.

The lifting condensation level is defined as the height where condensation would occur would an air parcel be lifted from the surface adiabatically and without mixing with the surrounding air. However, when a surface based inversion is present such an air parcel would not be very likely to get lifted to such altitudes. Any inversion between the starting point and the LCL would indeed stop the journey of the air parcel. The discrepancy between the LCL and the cloud base height is another indication that the P-MPC were mostly decoupled from the surface. Although these results are somewhat interesting, we do not think the LCL is such a relevant parameter for the considered cloud regime and therefore chose not to include it in the manuscript.

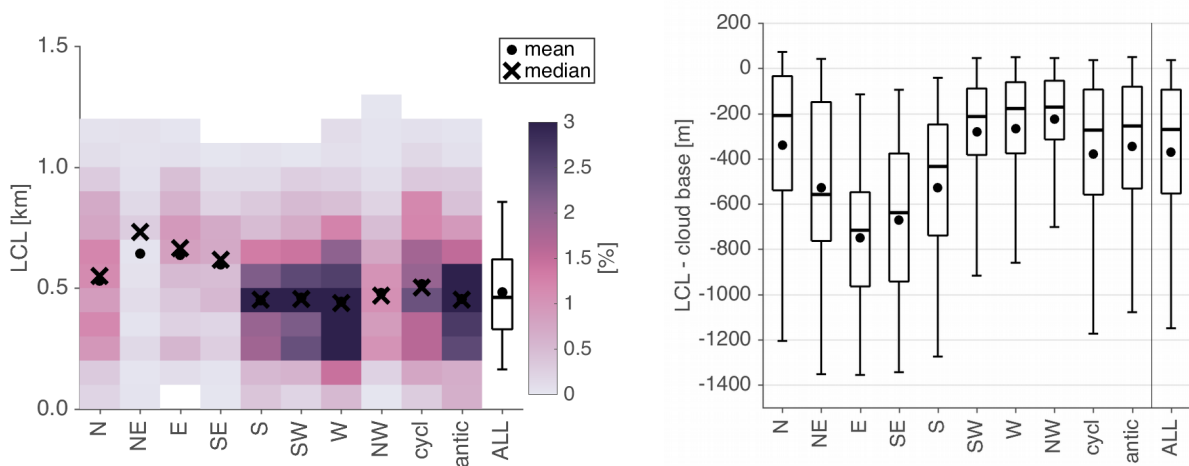


Figure IV. Lifting condensation level (LCL) for each weather type (left) and the difference between the LCL and cloud base (right) for all P-MPC.

L.325: As far as I understood, the results described here are the most important one in this study. The authors may need to explain more on the physics behind. Higher LWP can be due to higher temperature (thermodynamic effect), moisture transport, lower stability (geometrically thicker clouds) and others. The authors may describe how these factors affect LWP under the westerly conditions, using IWV data and from viewpoint of seasonality.

The referee is commenting on the statement “the westerly weather types (SW, W and NW) were associated with lower P-MPCs and with more liquid and ice (mean LWP 42 gm^{-2})”. As stated above in the response for comment number 1, we have added the consideration of atmospheric humidity and temperature to Sect. 4.2. As a response for comment number 2, seasonality of LWP as well as atmospheric humidity and temperature were included in Sect. 4.3.

Section 4.3: In my opinion, this section can be moved to appendix or deleted. Figure 9 clearly shows that 850 hPa wind direction is more important than that at surface. The addition of surface wind analyses did not provide enough insights into the P-MPC.

We understand that the referee did not find the section in question as relevant as the other sections. While the local winds did not provide many additional insights for the P-MPC specifically, the wind climate of Kongsfjorden is one of the features that makes Ny-Ålesund different from many other Arctic sites with long term cloud observations. We therefore consider it worthwhile to address the local wind conditions. We would also like to point out that while these results might not be that interesting for the wider Arctic mixed-phase cloud community, they are of interest for those working with data obtained at Ny-Ålesund. However, we recognize the critique of the referee, and correspondingly have moved the parts detailing the variation in P-

MPC properties to an appendix and only shortly summarize the main findings. Additionally, the figure and related discussion about the relationship between coupling and surface wind direction was moved to this section to shift the focus on the result related to the surface winds that we found most interesting.

Changes in the manuscript:

- The section was moved to the end of Sect. 4, and is now Sect. 4.5 *Local wind patterns around Ny-Ålesund*.
- Figure 10, L. 354-367 and L. 471-488 of the original manuscript were moved to the appendix A1 *P-MPC properties*. These results are summarized in the main text (L. 544-550) as follows:

“Regarding P-MPC properties, no strong relationships with surface wind direction were identified. Only the main findings are summarized here and further details are provided in Appendix A1. Considering weather types N, W and SW, which have the most cases across different surface wind directions, no statistically significant differences were found in the median liquid base height or cloud top temperature. The northwest surface wind was associated with the highest median LWP, possibly due to higher level of humidity available over the open sea. The southwest surface wind was associated with a significantly higher IWP for weather types W and SW (median IWP 16 gm⁻² and 18 gm⁻², respectively). However, these variations in LWP and IWP were not found for all three weather types analyzed.” (L. 540-546)
- The related conclusion was re-formulated and now states: “Local winds were not found to impact the occurrence or the height of the P-MPCs, but for some free-tropospheric wind directions the surface wind direction was related to variations in LWP and IWP.” (L. 582-584)
- Figure 11b, L. 385-386 and L. 503-507 of the original manuscript were moved to Sect. 4.5.

L.487: What is the “observed differences”?

We apologize the unclear writing. The “observed differences” simply referred to the differences presented in that section.

Changes in the manuscript:

“the observed differences in IWP and LWP” → “the differences found in IWP and LWP between different wind regimes” (L. 648-649)

L. 542: According to Nomokonova et al., (ACP2019), mean value of IWP of MPC was 164 gm⁻², while it was 12 gm⁻². Why the values are so different?

Nomokonova et al. (2019) included all profiles with a mixed-phase cloud layer, defined as both ice and liquid water identified in the same cloud layer. This includes amongst others deep and heavily precipitating cloud systems, clouds related with frontal passages and storms, and convective clouds associated with cold air outbreaks. Many of these clouds are mixed-phase and have a higher IWP than the persistent low-level MPC that are investigated in our study, which leads to a much higher mean IWP. For an example of a MPC not included in this work, see the cloud present 29 May 2018 18-01 UTC in Fig. 2.

L.544: Less and higher P-MPC-> Less frequent and higher cloud base height of P-MPC

Thank you for the better formulation.

Changes in the manuscript:

“Less and higher P-MPC” → “Less frequent P-MPC and with higher cloud base height“ (L. 580)

L.554: The words “weather type” and “wind regime” are used in this study. Describe as “wind direction at 850 hPa” etc, such as in figure captions for Figure 4b.

Changes in the manuscript:

We changed the wording of the corresponding sentence:

“The variation of median LWP between different **weather types** (Fig. 8b) was larger than the variation found between different **wind regimes** (Fig. 10b) or coupling states (Fig. 12a).”

changed to

“The variation of median LWP between different **wind direction at 850 hPa** was larger than the variation found between different **surface wind regimes** or coupling states.” (L. 587-589)

Reply to Referee #2

(1) Section 4 is mainly a description of statistics. No attempt to physically interpret these results is made before section 5. I would recommend to the authors to discuss the underlying physical processes and how these are supported by the statistics during section 4. It is hard to remember all the details of this section when reading the recap in section 5.

We thank the referee for this feedback and follow the recommendation.

Changes in the manuscript:

Sections 4 and 5 were merged and structured so that the relevant discussion is placed together with the presentation of the corresponding results. Sect. 4 is titled “*Results and discussion*” and now has thematic subsections.

(2) Seasonality is discussed in section 4.1 and regional wind patterns in section 4.2, but there is no attempt to investigate the links between these two factors. If a certain wind pattern dominates specific seasons, this should be considered when interpreting the results in section 4.2. The authors should present the frequency of the different wind patterns through the year.

The referee is correctly pointing out that the seasonality in persistent low-level mixed-phase cloud (P-MPC) occurrence together with a potential seasonal variation in regional wind direction should be considered when interpreting the results related to the connection between the P-MPC and wind direction. We have not found such seasonal variation in the weather type (used to describe the regional wind field at 850 hPa) that could explain the observed differences in cloud occurrence and properties between different weather types. To allow others to make the same conclusion, we have added a figure presenting the seasonal occurrence of all weather types (Fig. 10) in the manuscript.

Changes in the manuscript:

To clearly demonstrate that the dependency of P-MPC on weather types presented in Sect. 4.2 is not a result in seasonal variation of P-MPC occurrence and properties combined with a seasonality in 850 hPa wind direction, Fig. 10 is included in Sect. 4.3 with the following text:

“Since P-MPC properties (excluding LWP) as well as atmospheric temperature and humidity vary seasonally, a seasonal dependency in wind direction could explain the weather type dependent variations in P-MPC properties found in Sect. 4.2. To examine this possibility, Fig. 10 shows the proportion of P-MPC observations in each season for every weather type. The observation period of 2.5 years from June 2016 to October 2018 together with the seasonal variation in P-MPC occurrence (Fig. 5) lead to the uneven distribution of data between seasons. Overall, the summer months contribute most to the data set. However, there are no extensive differences found between the weather types. Most noteworthy is the high spring and low autumn occurrence of NW, which might contribute to the high IWP for this weather type (Fig. 7c). Furthermore, N and E were relatively more common in winter, N and SE more common in spring, and N less common in autumn. Given the lack of clear trends, we believe the seasonal variation in wind direction plays a minor role in the weather type dependent differences in P-MPC occurrence and properties described in the previous section.” (L. 416-425)

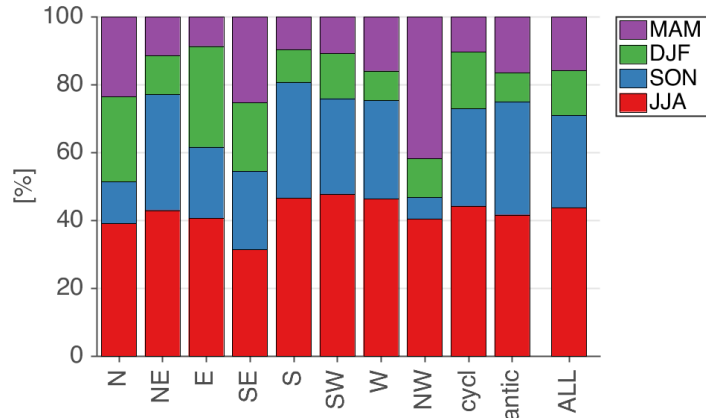


Figure 10. Distribution of seasons in the studied data set for each weather type. Only time periods when a P-MPC was present are included to evaluate the possible impact of wind direction seasonality on cloud properties and occurrence.

(3) When using the MWR θ -profile to assess decoupling, $\Delta\theta$ between the surface and the height half way to the liquid layer is estimated. But if decoupling occurs between this level and liquid base height, then the algorithm would classify a decoupled cloud as coupled. Do results vary significantly when using the gradient between the surface and the level exactly below the liquid layer as criterion? Please check the uncertainty in the applied method.

We first elaborate on the reasoning behind the choice made, as this was not made clear enough in the manuscript, before replying to the explicit comments/questions made.

Figures 3a and b (see below) show two example cases, one for a coupled and one for a decoupled cloud. Comparing the θ -profiles from sounding and MWR highlights the challenge of using the MWR data: While the general shape of the profile can be retrieved, it is not possible to resolve sharp inversions or detailed structures of the profile. Temperature inversions are very common at cloud top, and impact the accuracy of the potential temperature retrieved from MWR measurements in the vicinity of the inversion. Examining the profiles at liquid base in Fig. 3 and b reveals that the MWR profile is deviating from the sounding profile already at and below liquid base. Figure 3c presents a comparison of MWR profiles with all available soundings when a P-MPC was present confirming this issue being present in most of the cases. At 0.5*liquid base height the impact of cloud top inversion is not present like it is at liquid base, which is why we chose this height to determine the stability of the subcloud layer.

The method does not explicitly identify cloud decoupling, instead the stability of the lower half of the subcloud layer is estimated and used as a proxy for decoupling. If decoupling takes place above this layer, it is common for the lower half of the subcloud layer to

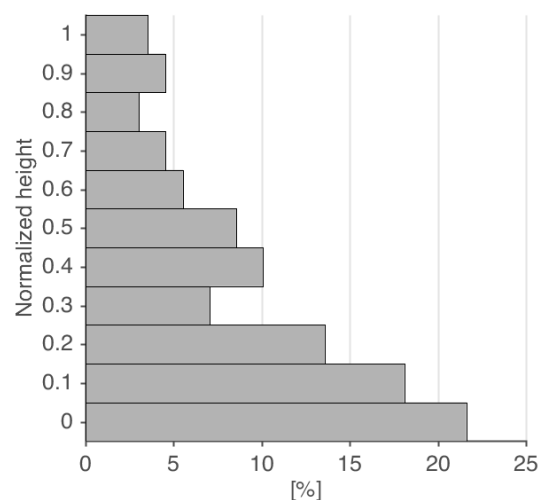


Figure V. Distribution of the surface based mixing layer height in the sounding profiles classified as decoupled (165 cases)

be at least partially stable leading to a correct identification of decoupling. The reviewer states that if decoupling happens above the $0.5 \times$ liquid base height, the cloud would be erroneously considered coupled. This is only true if additionally the layer from surface up to this height is well-mixed. We analysed the soundings classified as decoupled to investigate the depth of a surface based mixing layer using the same method as for detecting the decoupling but from surface upwards. The distribution of the surface based “mixing layer height, normalized to cloud base height, is shown in Fig. V. The figure confirms the commonality of a stable lower half of the subcloud layer for decoupled clouds, which aids the MWR based algorithm in detecting decoupling.

The referee is further asking if results vary significantly if the potential temperature at liquid base height is used. Using potential temperature at $0.5 \times$ liquid base height yields 77 % of all MWR profiles classified as decoupled. If we use liquid base height instead, 95 % of all MWR profiles become decoupled. The difference is clear, and the agreement with soundings is worse when using θ at the liquid base height.

Changes in the manuscript:

- Fig 3a was replaced with two example profiles, one for a coupled and one for a decoupled case. The main outcome of the original Fig. 3a was already included in the text, but was slightly extended:

“The resulting θ -profiles were compared with the profiles from radiosondes in the period June 2016–October 2018 (**Fig. 2a**). A slight cold bias is present, but in the lowest 2.5 km the RMSE is below 1.8 K”

changed to

“The resulting θ -profiles were compared with the profiles from radiosondes in the period June 2016–October 2018 (**not shown**). A slight cold bias is present (**< 0.4 K**). **The RMSE increases with altitude**, but in the lowest 2.5 km the RMSE is **still** below 1.8 K.” (L. 147-149)

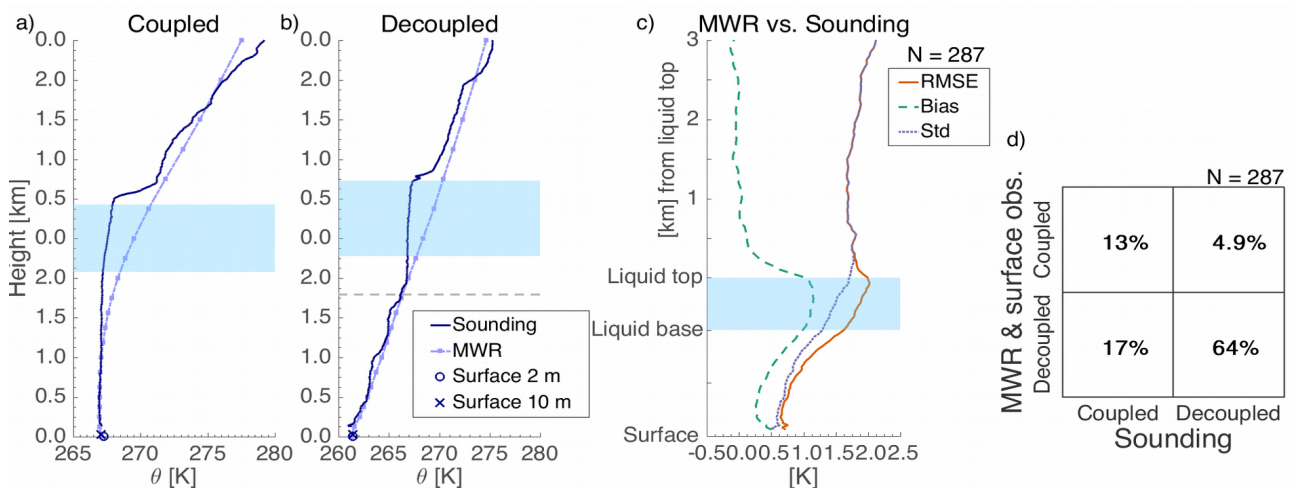


Figure 3. Examples of θ -profiles from sounding and MWR, as well as surface observations: a coupled cloud on the 24 October 2017 (a) and a decoupled cloud on the 1 February 2018 (b). The blue shaded area indicates the cloud layer, where cloud base and top are determined as the median values of the Cloudnet based cloud base and top for the duration of the sounding. The gray dashed line indicates the decoupling height defined from the sounding θ -profile. Comparison of potential temperature profiles from sounding and retrieved from MWR measurements when P-MPC were present, with height normalized in respect to the liquid layer (c). Comparison of the diagnosed coupling with the new method based on MWR and surface observations and based on sounding profiles (d).

- To accompany the new figures (Fig 3. and b), the following text was added:
 “Fig. 3 a and b show two example cases, one for a coupled and one for a decoupled cloud, respectively. Both profiles demonstrate a structure typical for stratiform Arctic MPC a temperature inversion at cloud top, below which a well mixed layer is identifiable. In the case of the coupled P-MPC (Fig. 3a), the well-mixed layer extends to the surface. For the decoupled P-MPC (Fig. 3b) the well-mixed layer extends 200 m below the liquid layer base, below which several weaker temperature inversions and a generally stable stratification can be identified.” (L. 190-194)
- The reasoning for the use of half of the liquid base height was extended, and is now:
 “The reason for using the height equalling half of the liquid layer base height can be understood by comparing the θ -profiles from sounding and MWR in Fig. 3 a and b. While the general shape of the profile can be retrieved from the MWR measurements, it is not possible to resolve sharp inversions or detailed structures of the profile. Yet temperature inversions are very common at the top of P-MPCs. The comparison of MWR profiles with all available soundings when a P-MPC was present (Fig. 3c) shows that the accuracy of the retrieved potential temperature is reduced in the vicinity of the liquid layer top and that the influence extends to below the liquid layer base. At 0.5*liquid base height the impact of cloud top inversion is smaller than at liquid base and the RMSE is below 1 K, which is why we chose this height to determine the stability of the subcloud layer. Note, that it should not be inferred that the method can only detect decoupling occurring in the lowest half of the subcloud layer. When decoupling occurs above the layer explicitly included, it is common that the lower half of the subcloud layer is at least partly stably stratified, as can also be seen in the example of Fig 3b, prompting a correct decoupling classification.” (L. 206-216)

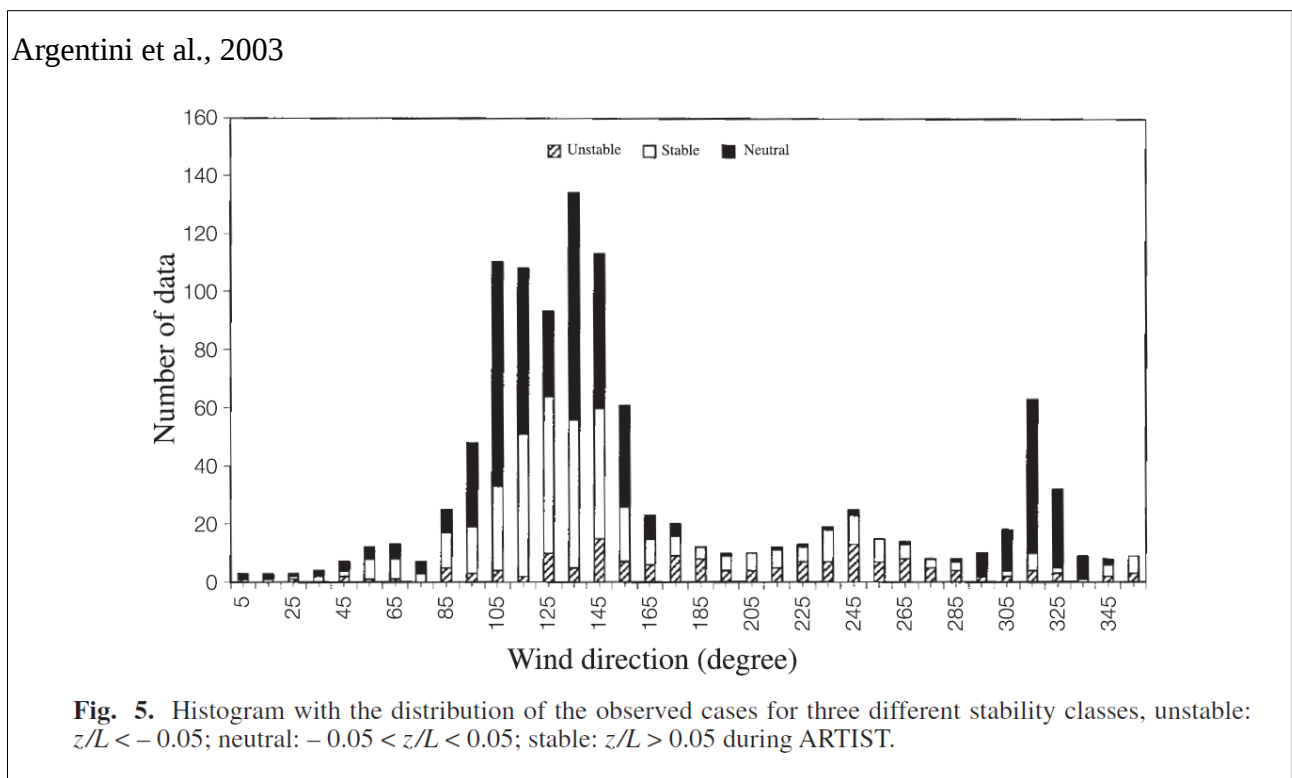
(4) A main conclusion is that cloud-surface coupling is more frequent when wind comes from the sea and that it enhances cloud liquid. However for these conditions coupling occurs for somewhat less than 50 % of the time. I suggest to the authors to investigate the meteorological conditions (e.g. large-scale moisture transport) between the decoupled and coupled cases when NW surface winds prevail. This might give indications of what drives coupling, which I don't think is the local wind pattern.

The referee is questioning two conclusions drawn from the analysis, firstly that the local wind pattern drives cloud-surface coupling, and secondly, that coupling with northwesterly surface wind enhances cloud liquid. We address both concerns individually.

Considering the relationship between surface coupling of P-MPC and the local wind patterns, we found that the frequency of coupling clearly varied between the different surface wind direction modes (Fig. 13b). This relationship was present in all seasons, although weaker in summer despite the seasonal variation in the surface wind (Fig. A2). However, we do not believe that the local wind patterns, approximated here by the surface wind direction, are the only factor determining the coupling of the cloud. The depth of the cloud driven mixing layer (which depends on both the generation of turbulence and the stratification of the adjacent layers) as well as the proximity of the cloud to the surface are both factors for the coupling of the cloud. However, based on our work and that of others, we believe there is evidence that the local winds associated with glacier outflows can act against the coupling of a cloud. In the literature the southeast and southwest surface winds have been associated with katabatically driven flows from the nearby glaciers (Beine et al., 2001; Jocher et al., 2012; Argentini et al., 2003). Beine et al. argued that the northwest surface wind in summer is related to sea breeze. Argentini et al. evaluated the stability as a function of wind direction during the ARTIST campaign (15 March – 16 April 1998 at Ny-Ålesund). Fig. 5 in Argentini et al. 2003 (see below) shows that stable conditions were mainly observed with southeast surface wind and hardly ever with northwest wind. Unstable conditions occurred from 90° to 270° and under light wind conditions. Furthermore, they found large wind shear to generate turbulence and lead to neutral stratification. The

katabatic flows bring cold air down to the valley in a shallow layer close to the surface (Beine et al. 2001). In our opinion, such a cold surface layer would be efficient in decoupling the cloud above.

The hypothesis that glacier outflows act to decouple the P-MPC is based on the results in previous studies about modifications in the surface layer related to the local winds, and supported by the results we found in our study, namely Fig. 13b and A2. The manuscript in its original form required perhaps too much foreknowledge on the Kongsfjorden wind conditions for the argumentation to be clear. We have therefore extended the description of local wind conditions at Ny-Ålesund as well as the discussion related to these results to better explain our argumentation. Furthermore, we added the seasonality of the surface wind direction and associated coupling frequency in the appendix (Sect. A2) to provide a well rounded description of the surface wind conditions.



For the second point related to the relationship between coupling and cloud liquid in P-MPC for northwesterly surface wind, we agree that the result was overemphasized. As pointed out by the referee, further analysis would be required to determine which processes are important for this subset of P-MPC cases. However, we find this additional work would be beyond the scope of this paper. While we still consider it worthwhile to point out the possible relationships between coupling, surface wind direction and amount of liquid in P-MPC, we have removed the corresponding statements from the conclusions and abstract of the paper.

Changes in the manuscript

- The description of the local wind climate in Sect. 3.4 was extended with a new paragraph summarizing previous studies:
 “The channeling of the free-tropospheric wind along the fjord axis is a typical feature of an Arctic fjord (Svendsen et al., 2002; Esau and Repina, 2012, and references therein). Previous work has found the feature prominent also at Kongsfjorden (Maturilli and Kayser, 2017). It is well documented that despite the dominating westerly free-tropospheric wind direction, in Kongsfjorden the near surface wind tends to blow southeasterly along the fjord axis (Maturilli and Kayser, 2017;

Beine et al., 2001; Jocher et al., 2012). This is usually attributed to katabatic forcing of the Kongsvegen glacier about 15 km east-southeast from Ny-Ålesund (Fig. 1), although Esau and Repina (2012) argued that for typical synoptic conditions the land-sea breeze circulation would be the dominant driver. The secondary mode in surface wind is from northwest, from the sea towards the island's interior. According to Jocher et al. (2012) the northwesterly surface winds are associated to cold air advection that relate to passing low-pressure systems. Beine et al. (2001) find this wind direction to be pronounced in June and July, which they associate with sea breeze and the melting of sea ice. In addition, at Ny-Ålesund weak southwesterly surface winds are observed, caused by katabatic flow from the Zeppelin mountain range and the Broggerbreen glacier south of Ny-Ålesund (Jocher et al., 2012; Beine et al., 2001) under specific synoptic conditions (Jocher et al., 2012; Argentini et al., 2003). The local wind conditions impact the stratification of the local boundary layer (Argentini et al., 2003; Svendsen et al., 2002). Argentini et al. show that during the ARTIST campaign (15 March – 16 April 1998 at Ny-Ålesund) stable conditions were mainly observed with southeast wind and hardly ever with northwest wind. Unstable conditions occurred from 90° to 270° and under light wind conditions. Furthermore, large wind shear was observed to generate turbulence and lead to neutral stratification. This brief summary of previous studies demonstrates the complexities of the local wind conditions present at the AWIPEV station.” (L. 244-261)

- Because of the additional description of the local wind field based on literature, we removed some of the description of the wind conditions based on presented data. Specifically, the second example of the wind direction profiles, Fig. 5b of the original manuscript, was removed. The description of the wind profiles from the presented soundings was shortened. Figure 5a was combined with Fig. 4 and is Fig 5a has become Fig 4c in the revised manuscript.
- The discussion on the relationship between surface wind direction and coupling was extended to better explain the mechanisms in play:

“Local winds in Kongsfjorden were quite apparently connected to the coupling of the P-MPC (Fig. 13b). Coupling was most common with northwest surface wind (from the sea) and least common with the southeast surface wind (towards the sea), and the same behaviour was found for every season despite the seasonality of both surface wind direction and cloud coupling (see Appendix A2). For the P-MPC to be thermodynamically decoupled from the surface, a stably stratified layer needs to exist between the surface and the cloud base. Argentini et al. report a dependence of surface layer stratification on wind direction (Argentini et al., 2003, Fig. 5). Stable conditions were most often found with southeast surface wind, for which only 8% of the P-MPC were considered coupled. On the other hand, stable conditions were rare with northwest surface wind, for which 37% of the P-MPC were coupled. The near surface wind from southwest and southeast is often related with flows from the glaciers (Jocher et al. 2012; Beine et al. 2001; Sect. 3.4) that bring cold air down to the valley in a shallow layer close to the surface. Such a cold surface layer is very efficient in decoupling the cloud and acts against the cloud driven turbulence that could otherwise couple the P-MPC to the surface. This effect might be stronger with southeast than southwest surface wind, since the katabatic winds from southwest are weaker (Fig. 4a). The differences in the coupling of the P-MPC with varying wind conditions can be explained by the differences in stratification of the lower boundary layer under different surface wind conditions. We conclude that the surface wind has the potential to modify the conditions in the boundary layer, which in turn can act to suppress coupling.” (L. 547-561)
- Added Appendix A2 *Seasonality of surface wind direction and P-MPC coupling*, describing the seasonal variation in surface wind direction and the relationship with wind direction and P-MPC coupling. For complete text see the attached manuscript.

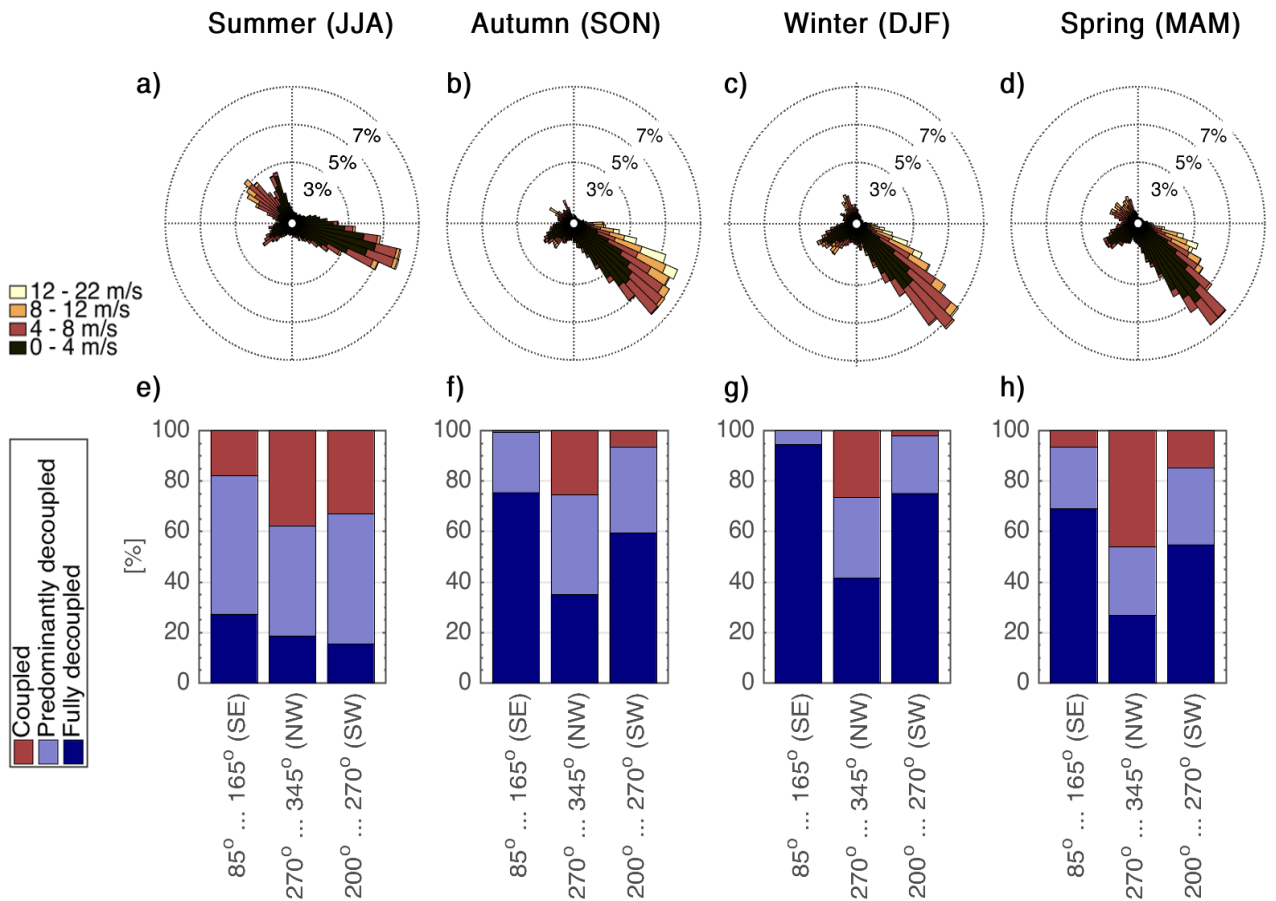


Figure A2. Wind rose for 30 min mean 10 m wind for each season (a-d) in the cloud observation period (June 2016--October 2018). The fraction of P-MPC cases classified as coupled, predominantly decoupled and fully decoupled for each surface wind direction mode in each season (e-f).

- Removed from conclusions: “Some of the observed differences between different wind regimes and coupling states might have been related (e.g. higher LWP were found for coupled P-MPC and for P-MPC associated with northwest surface wind, while coupling was most common for this surface wind direction).”
- Removed from abstract: “Furthermore, the near surface wind direction from the open sea was related to higher amounts of cloud liquid, and higher likelihood of coupling.”
- Added at the end of Sect. 4.5 *Local wind patterns around Ny-Ålesund*: “There is a relationship between surface coupling and the local wind conditions at Ny-Ålesund, but to understand the impact of the combined effects on P-MPC properties would require further studies.” (L. 569-570)

Abstract: it is stated that westerly clouds had a higher mean liquid (42 gm^{-2}) and ice water path (16 gm^{-2}) compared to the overall mean of 35 and 12 gm^{-2} , respectively. Is a 7 gm^{-2} difference in LWP important, given the large uncertainty in these retrievals? Moreover, I doubt that the impact on radiation is substantially different when changing cloud LWP by 7 gm^{-2} . I don't think differences of this magnitude should be emphasized in the text.

The referee argues that the abstract mistakenly emphasizes the differences between P-MPC associated with westerly winds and all P-MPC. We agreed that this was not formulated correctly.

Changes in the manuscript:

“We found that persistent MPCs were most common with westerly winds, and the westerly clouds had a higher mean liquid (42 gm^{-2}) and ice water path (16 gm^{-2}) **compared to the overall mean of 35 and 12 gm^{-2} , respectively.**” (L. 8-9)

changed to

“We found that persistent low-level MPCs were most common with westerly winds, and the westerly clouds had a higher mean liquid (42 gm^{-2}) and ice water path (16 gm^{-2}) **compared to those with easterly winds.**” (L. 8-9)

Sections 2.3 and 3.3 offer a summary of the methods used to study the influence of the large-scale and the local wind patterns, respectively. However the first method is included in Section 2 (Observations) and the second in Section 3. It would make more sense if section 2.3 becomes a subsection of Section 3, too.

We agree, and thank for the suggestion.

Changes in the manuscript:

Section 2.3 *Circulation weather type* was moved to Sect. 3.

Section 4.1: The percentages given in this section would be more meaningful if the actual number of PMPCs and all-PMC cases included in the analysis is stated. Is it same as in Figure 2?

The criteria for identifying P-MPC is given in detail in Sect. 3.1. Because our interest was in persistent MPCs, one important case selection criteria was the condition for an liquid layer uninterrupted for at least 1h. The ‘P-MPC case’ is defined from the beginning to the end of the occurrence of the persistent liquid layer. The total number of these cases was 1412. The number given in Fig. 2 (Fig. 3 in the revised manuscript) refers to the number of sounding profiles that coincide with a P-MPC and when MWR data was available. The all-MPC occurrence refers to 30 second profiles that include co-existing liquid and ice. The total number of such profiles is 985901. Cases have not been identified for the all-MPC in the same sense as for the P-MPC. This is also mentioned in the text: “The ‘all MPC’ and the P-MPC occurrences in Fig. 5 are not directly comparable, since the first one refers to individual profiles and the latter is to a large extent defined by a temporally continuous liquid layer and also includes profiles without a mixed-phase layer detected” (L. 317-319).

Changes in the manuscript:

- Added in Sect. 4.1: “In total 1412 cases of P-MPC were identified.” (L. 317)
- To clarify that the cloud occurrence statistics is based on the 30 s profiles, this is now mentioned when the results are introduced:
“We first examine the frequency of occurrence of different types of clouds in the observation period of the cloud radar (10 June 2016–8 October 2018) **considering the 30 s averaged columns of the Cloudnet product.**” (L. 303-304)

L300-302: how different are the occurrence statistics in the sensitivity test?

Changing the longest allowed gap in the liquid layer from 5 to 2 min decreases the cases detected from 1412 to 1235. The fraction of P-MPC in the total data set decreases from 23% to 19%. Figure VI shows the monthly differences. Overall, using a stricter criteria shrinks the dataset.

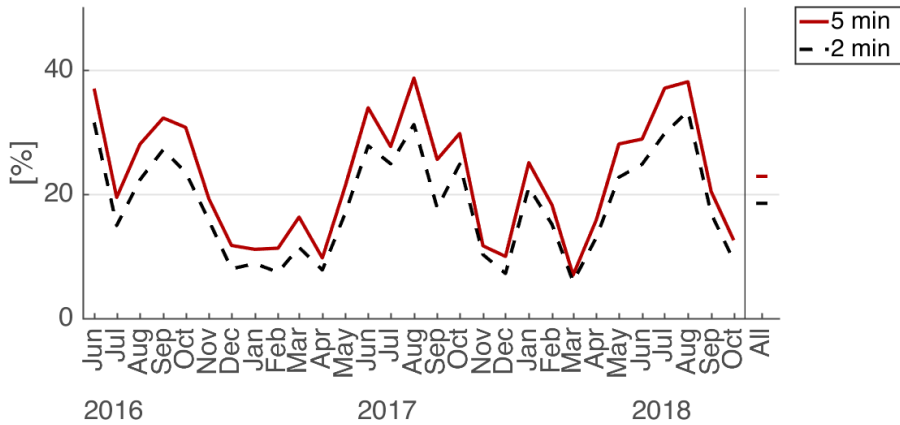


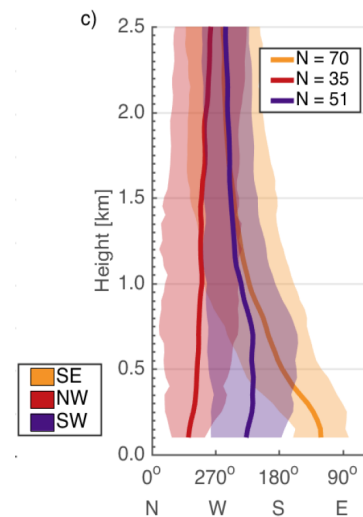
Figure VI. Frequency of occurrence of P-MPC, allowing a maximum gap in the liquid layer to be 5 or 2 min in the P-MPC identification algorithm.

L481-484: here you combine Figure 5 and 10a to discuss how wind structure affects the PMPCs. However, Figure 5 corresponds to a much longer period than Figure 10a. For consistency, both wind and cloud measurements should correspond to the same time. Please check if utilizing fewer radiosondes results in very different wind structures. If this is the case, then you might consider removing/modifying the relevant discussion.

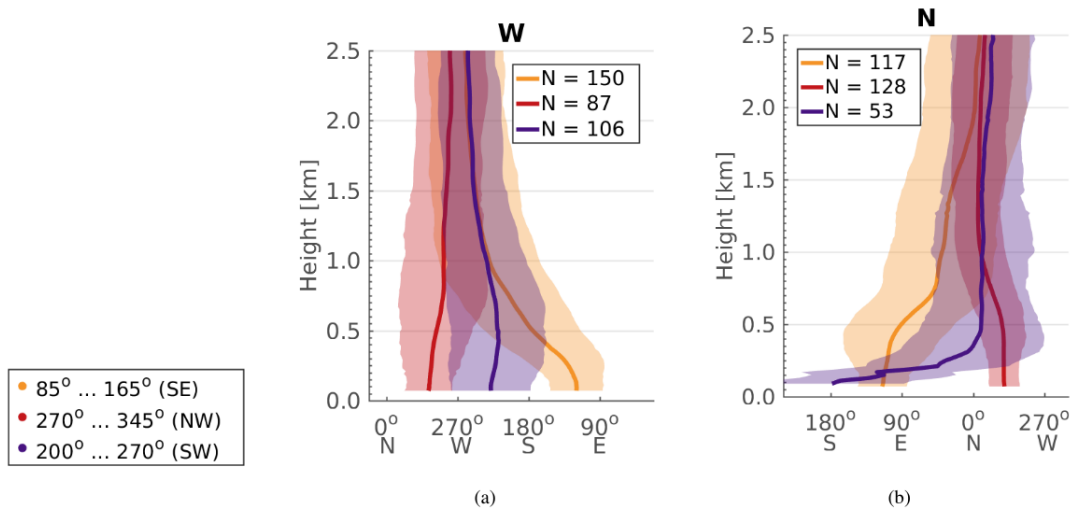
The referee expresses concerns that mistaken conclusions might be made because Fig. 5 includes the time period August 2011 – October 2018, when all other analysis were focused on the period June 2016 – October 2018. Here we show Fig. 4c (corresponding to Fig. 5a) that includes data only for the cloud observation period, June 2016 – October 2018. The original Fig. 5 is also included here (see below) for comparison. We appreciate the advice from the referee and for consistency changed the figure in the manuscript to only include the cloud observation period.

Changes in the manuscript:

- The figure in question (Fig. 4c in the revised manuscript) was updated to only include soundings from the cloud observation period (June 2016 – October 2018).



Updated Fig. 5a (Fig 4c in the revised manuscript) based on radiosoundings from June 2016 to October 2018.



Original Fig. 5 based on radiosoundings from August 2011 to October 2018.

Figure 6: it would be better if the actual number of profiles is also included in the figure.

The referee is suggesting to include the number of profiles in Fig. 5 of the revised manuscript. Unfortunately it is not possible to add the number of profiles in the figure, the only option would be to redo the figure using the number of profiles instead of relative frequencies. This is because the figure shows monthly values, and different months have different number of days, yielding to different number of profiles for the same frequency of occurrence in different months. Therefore we believe it would be misleading to use the number of profiles instead of the relative occurrence, as suggested by the referee.

Figure 9: the size of the dots

Done.

References

- Argentini, S., Viola, A. P., Mastrantonio, G., Maurizi, A., Georgiadis, T., and Nardino, M.: Characteristics of the boundary layer at Ny-Ålesund in the Arctic during the ARTIST field experiment, *Annals of Geophysics*, 46, 2003.
- Beine, H., Argentini, S., Maurizi, A., Mastrantonio, G., and Viola, A.: The local wind field at Ny-Ålesund and the Zeppelin mountain at Svalbard, *Meteorol. Atmos. Phys.*, 78, 107–113, 2001.
- Dahlke, S. and Maturilli, M.: Contribution of Atmospheric Advection to the Amplified Winter Warming in the Arctic North Atlantic Region, *Adv. Meteorol.*, 2017, 2017.
- Jocher, G., Karner, F., Ritter, C., Neuber, R., Dethloff, K., Obleitner, F., Reuder, J., and Foken, T.: The near-surface small-scale spatial and temporal variability of sensible and latent heat exchange in the Svalbard region: a case study, *ISRN Meteorology*, 2012, 2012.
- Stull, R. B.: *An introduction to boundary layer meteorology*, vol. 13, Springer Science & Business Media, 1988.

Low-level mixed-phase clouds in a complex Arctic environment

Rosa Gierens¹, Stefan Kneifel¹, Matthew D. Shupe^{2,3}, Kerstin Ebell¹, Marion Maturilli⁴, and Ulrich Löhnert¹

¹Institute for Geophysics and Meteorology, University of Cologne

²Cooperative Institute for Research in Environmental Science, University of Colorado

³NOAA Earth System Research Laboratory, Physical Science Division

⁴Alfred Wegener Institute Helmholtz Centre for Polar and Marine Research, Potsdam, Germany

Correspondence: Rosa Gierens (rgierens@uni-koeln.de)

Abstract.

Low-level mixed-phase clouds (MPC) are common in the Arctic. Both local and large scale phenomena influence the properties and lifetime of ~~MPC~~MPCs. Arctic fjords are characterized by complex terrain and large variations in surface properties. Yet, not many studies have investigated the impact of local boundary layer dynamics and their relative importance on ~~MPC~~MPCs in the fjord environment. In this work, we used a combination of ground-based remote sensing instruments, surface meteorological observations, radiosoundings, and reanalysis data to study persistent low-level ~~MPC at Ny-Ålesund~~MPCs at Ny-Ålesund, Svalbard, for a 2.5 year period. Methods to identify the cloud regime, surface coupling, as well as regional and local wind patterns were developed. We found that persistent low-level MPCs were most common with westerly winds, and the westerly clouds had a higher mean liquid (42 gm^{-2}) and ice water path (16 gm^{-2}) compared to ~~the overall mean of 35 and 12,~~
10 ~~respectively~~those with easterly winds. The increased height and rarity of persistent MPCs with easterly free-tropospheric winds suggest the island and its orography have an influence on the studied clouds. Seasonal variation of the liquid water path was found to be minimal, although the occurrence of persistent MPCs, their height and ice water path all showed notable seasonal dependency. Most of the studied MPCs were decoupled from the surface (63–82 % of the time). The coupled clouds had
15 41 % higher liquid water path than the fully decoupled ones. Local winds in the fjord were related to the frequency of surface coupling, and we propose that katabatic winds from the glaciers in the vicinity of the station may cause clouds to decouple.
~~Furthermore, the near-surface wind direction from the open sea was related to higher amounts of cloud liquid, and higher likelihood of coupling.~~We concluded that while the regional to large scale wind direction was important for the persistent MPC occurrence and ~~its~~ properties, also the local scale phenomena (local wind patterns in the fjord and surface coupling) had an influence. Moreover, this suggests that local boundary layer processes should be described in models in order to present
20 low-level MPC properties accurately.

1 Introduction

The Arctic is warming more rapidly than any other ~~areas~~area on Earth due to climate change (Serreze et al., 2009; Solomon et al., 2007; Wendish et al., 2017). It is well established that clouds strongly impact the surface energy budget in the Arctic

(Dong et al., 2010; Shupe and Intrieri, 2004), but feedback processes that include clouds are not well characterized (Choi et al., 2014; Kay and Gettelman, 2009; Serreze and Barry, 2011). Particularly low-level mixed-phase clouds are important for the warming of near-surface air (Shupe and Intrieri, 2004; Intrieri et al., 2002; Zuidema et al., 2005). The multitude of micro-physical and dynamical processes within the cloud and the interactions with local and large scale processes make these mixed-phase clouds difficult to represent in numerical models (Morrison et al., 2008, 2012; Komurcu et al., 2014). Improvements in the process-level understanding are still required to improve the description of low-level mixed-phase clouds in climate models (McCoy et al., 2016; Kay et al., 2016; Klein et al., 2009).

Previous studies have shown the prevalence of mixed-phase clouds (MPC) across the Arctic (Shupe, 2011; Mioche et al., 2015). MPCs occur in every season, with the highest occurrence in autumn and in the lowest 1 km above the surface, and can persist from hours to days (Shupe et al., 2006; Shupe, 2011; De Boer et al., 2009). The persistent low-level MPCs have a typical structure that consists of one or more super-cooled liquid layers embedded in a deeper layer of ice, where liquid is usually found at cloud top and the ice precipitating from the cloud may sublime before reaching the ground (Morrison et al., 2012, and references therein). Several studies have shown an increase in cloud ice to coincide with increase in cloud liquid, suggesting that ice production is linked to the liquid water in the cloud (Korolev and Isaac, 2003; Shupe et al., 2004, 2008, 2006; Westbrook and Illingworth, 2011; Morrison et al., 2005). The amount of liquid and ice, and the partitioning between the condensed phases (i.e., phase-partitioning), are important parameters due to their key role in determining the clouds' radiative effect (Shupe and Intrieri, 2004).

A variety of environmental conditions can effect cloud micro- and macro-physical properties. According to simulations over different surface types, changes in surface properties lead to changes in the thermodynamic structure of the atmospheric boundary layer, the extent of dynamical coupling of the cloud to the surface, as well as the micro-physical properties of the MPC (~~Morrison et al., 2008; Li et al., 2017; Savre et al., 2015~~)([Morrison et al., 2008; Li et al., 2017; Savre et al., 2015; Eirund et al., 2019](#)).

Also observational evidence on the connection between changes in surface conditions and MPC occurrence (Morrison et al., 2018) as well as thermodynamic structure and droplet number concentration (Young et al., 2016) have been found. Kalesse et al. (2016) discovered in a detailed case study that for the MPC in question, phase partitioning was affected by the coupling of the cloud to the surface, large scale advection of different airmasses as well as local scale dynamics. On the contrary, Sotiropoulou et al. (2014) did not find differences in cloud water properties between coupled and decoupled clouds. Scott and Lubin (2016) show that at Ross Island, Antarctica, orographic lifting of marine air is likely causing thick MPCs with high ice water content. Changes in aerosol population, especially ice nucleating particles (INP), have been found to modulate the ice formation rate (Jackson et al., 2012; Morrison et al., 2008; Norgren et al., 2018; Solomon et al., 2018). To complicate matters further, the cloud also modifies the boundary layer where it resides by modifying radiative fluxes, generating turbulence (due to cloud top cooling), and vertically redistributing moisture (Morrison et al., 2012; Solomon et al., 2014; Brooks et al., 2017).

While being common in the entire Arctic, ~~MPC~~[MPCs](#) are most frequently observed in the area around Svalbard and the Norwegian and Greenland seas (Mioche et al., 2015). Nomokonova et al. (2019b) report one year of ground based remote sensing observations of clouds at Ny-Ålesund, Svalbard, and find that 20 % of the time single-layer MPCs (defined as single-layer clouds with ice and liquid occurring at any height of the cloud) were present, with highest frequency in autumn and in

late spring/early summer. Svalbard lies in a region where intrusions of warm and moist air from lower latitudes are common (Woods et al., 2013; Pithan et al., 2018), and differences in air mass properties have been associated with differences in ice and liquid water content and particle number concentration in MPCs (Mioche et al., 2017). Locally, the archipelago exhibits large variations in surface properties (glaciers, seasonal sea-ice and snow cover) as well as orography. There are less MPCs over the islands than over the surrounding sea during winter and spring, while during summer and autumn the differences are small (Mioche et al., 2015), indicating that the islands modify the local boundary layer and the associated clouds. How the orography influences the low MPC-MPCs in more detail is difficult to study using space-born radars due to the rather big blind zone and considerably large footprint. Aircraft and ground-based remote sensing, together with modelling studies, are better suited for answering this question.

In this paper we investigate persistent low-level mixed-phase clouds (P-MPC) observed above Ny-Ålesund on the west coast of Svalbard. Mountainous coastlines are common at Svalbard, Greenland, and elsewhere in the Arctic (Esau and Repina, 2012); and Ny-Ålesund is an excellent site to study low-level MPCs in such complex environments. The time period considered is June 2016–October 2018, when a cloud radar of the University of Cologne was operating at the French–German Arctic Research Base AWIPEV as part of the project Arctic Amplification: Climate Relevant Atmospheric and Surface Processes, and Feedback Mechanisms (AC)³. A combination of ground based remote sensing instruments, surface meteorological observations, radiosoundings, and reanalysis data was used to identify and characterize the P-MPCs, to describe the extent of surface coupling, and to evaluate these in the context of wind direction in the area around the station. In addition to providing a description of micro- and macro-physical properties of P-MPC P-MPCs and their seasonal variation, we aim to identify some of the impacts the coastal location and the mountains have on the observed P-MPC P-MPCs, as well as determine the relevance of surface coupling for cloud properties at the site. In Sect. 2 the measurement site, the instrumentation and data products used are introduced, followed by the description of the methodology developed to identify persistent low-level MPC-MPCs (Sect. 3.1), coupling of the cloud to the surface (Sect. 3.2), and the approach to describe regional and local wind conditions (Sect. 3.3 and 3.4). The result section (Sect. 4) results and discussion section describes the occurrence of P-MPC (Sect. 4.1) and their average properties as well as variation under different conditions (regional and local wind direction, degree of coupling to the surface). At the end the different aspects are considered together to provide a description of P-MPC seasons and dynamical conditions. The relationship between P-MPC and the regional wind direction (Sect. 4.2), different seasons (Sect. 4.3), surface coupling (Sect. 4.4) as well as local wind conditions (Sect. 4.5) are considered. The results are discussed in the context of atmospheric temperature and humidity and considering previous studies at Ny-Ålesund (Sect. 5), followed by a short summary and other Arctic sites. In the end the main aspects are summarized followed by conclusions in Sect. 5.

2 Observations

2.1 Measurement site

The measurements were carried out at the French–German Arctic Research Base AWIPEV in Ny-Ålesund (78.9°N, 11.9°E), located on the west coast of Svalbard, at the south side of Kongsfjorden (Fig. 1). The area is mountainous, featuring seasonal

snow cover, a typical tundra system, and glaciers. In the period investigated the sea has remained ice-free throughout the year. The local boundary layer is known to be strongly affected by the orography (Kayser et al., 2017; Beine et al., 2001), and is often quite shallow with an average mixing layer height below 700 m (Dekhtyareva et al., 2018; Chang et al., 2017). Surface layer temperature inversions are common, especially in winter (Maturilli and Kayser, 2017). The mountains reach up to 800 m, and strongly influence the wind around Ny-Ålesund. In the free troposphere westerly winds prevail. The wind conditions are described more in detail in Sect. 3.4. Clouds have been found to occur above Ny-Ålesund 60–80 % of the time (Nomokonova et al., 2019b; Maturilli and Ebell, 2018; Shupe et al., 2011). ~~The inter-annual variability is large, however, clouds~~ Clouds generally occur more frequently in summer and autumn and are less common in spring, although the inter-annual variability is large.

2.2 Measurements and data products

Most of the measurements and cloud and thermodynamic parameter retrievals utilized were described in detail by Nomokonova et al. (2019b), and references therein. Here, the most important aspects are summarized, together with additional data products used. A summary of the instrumentation, their specifications and derived parameters is given in Table 1.

2.2.1 Instrumentation

We employ a suite of remote sensing instruments: radar, microwave radiometer and ceilometer. Within the frame of the (AC)³-project the JOYRAD-94 cloud radar was installed at AWIPEV on June 2016. In July 2017 it was replaced by the MIRAC-A cloud radar, which operated until October 2018. Both instruments are frequency modulated continuous wave cloud radars measuring at 94 GHz, described in detail by Kuchler et al. (2017). The main difference between the two radars is the size of the antenna, which for MIRAC-A is only half of that of the JOYRAD-94. The smaller antenna leads to a sensitivity loss of about 6 dB and an increase of the beam width from 0.53° to 0.85° (~~Meeh et al., 2019b~~)(Meeh et al., 2019a). A Humidity and Temperature PROfiler (HATPRO) passive microwave radiometer (MWR) has been operated continuously at AWIPEV since 2011. The instrument has 14 channels in the K- and V-bands to retrieve liquid water path (LWP), integrated water vapor (IWV), and temperature and humidity profiles (Rose et al., 2005). In addition to the zenith pointing measurements, an elevation scan is performed every 15–20 min to obtain more accurate temperature measurement in the boundary layer (Crewell and Löhnert, 2007). Finally, the Vaisala CL51 ceilometer measures at 905 nm providing attenuated backscatter coefficient (β) profiles (Maturilli and Ebell, 2018).

To compliment the remote sensing observations, we make use of soundings and standard meteorological parameters measured at the surface. In Ny-Ålesund radiosondes are launched routinely every day at 11 UTC, and more often during campaigns (Maturilli and Kayser, 2017; Dahlke and Maturilli, 2017). From the surface measurements we utilized temperature, pressure as well as wind speed and direction data (technical details in Table 1). The instruments for surface meteorology are continuously maintained by the AWIPEV staff, and all data is quality controlled (Maturilli et al., 2013).

2.2.2 Cloudnet

The Cloudnet algorithm combines radar, radiometer, and ceilometer with thermodynamic profiles from a numerical weather prediction (NWP) model to provide best estimates of cloud properties (Illingworth et al., 2007). The observational data, described in the previous section, is homogenized to a common resolution of 30 s in time and 20 m in the vertical. In the Ny-Ålesund dataset, the Global Data Assimilation System 1 (GDAS1, more info at <https://www.ready.noaa.gov/gdas1.php>) was used as the NWP model until the end of January 2017, after which it was replaced by the operational version of the ICON (ICOsahedral Non-hydrostatic) NWP model (Zängl et al., 2015).

In our work we rely on the target classification product (Hogan and O'Connor, 2004), that classifies objects detected in the atmosphere as aerosols, insects, or different types of hydrometeors (cloud droplets, drizzle, rain, ice, melting ice; see Fig. 2 for an example). Radar reflectivity (Z_e) and ceilometer β -profiles are used to detect the presence and boundaries of clouds. Cloud phase is distinguished on the basis of Z_e , β , temperature (T) and wet bulb temperature; in addition, Doppler velocity from radar is used to position the melting layer. No differentiation is made between ice in a cloud and precipitating ice. While applying this widely accepted methodology, for our study there are two important limitations. Firstly, the detection of liquid within a MPC is based on β , such that if cloud top is not found within 300 m from the height where the ceilometer signal is extinguished, all cloudy bins above this height are classified as ice. Secondly, no method to distinguish super-cooled drizzle from ice is available yet (Hogan et al., 2001; Hogan and O'Connor, 2004).

2.2.3 Derived properties

The amount of liquid and ice in the cloud, and their ratio, is one of the most important properties of MPCs. In addition, humidity supply is a key requirement for cloud formation and continuation. Liquid water path (LWP) ~~was~~ and integrated water vapor (I WV) were retrieved from the zenith-pointing observations of the MWR using statistical multi-variate linear regression (Löhnert and Crewell, 2003). Coefficients for the retrieval were based on sounding data; more details about the retrieval and corrections applied are given by Nomokonova et al. (2019b). Previous studies have found the accuracy of the method to be 20–25 gm^{-2} (Löhnert and Crewell, 2003).

Ice water content (IWC) was calculated using the Z_e - T -relationship from Hogan et al. (2006), where temperature was taken from the same model as used for Cloudnet. The uncertainty of the retrieval ~~was~~ is estimated to be -33–+50 % for temperatures above -20°C . Ice water path (IWP) for P-MPCs was calculated by integrating IWC from the surface to cloud top. Furthermore, the LWP was averaged to 30 s to match the temporal resolution of IWP.

In order to calculate the potential temperature (θ) profile based on the temperature profile retrieved from the MWR elevation scans, an estimate of the pressure profile is required. For this we took the measured surface pressure, and used the barometric height formula to estimate pressure at each height. The resulting θ -profiles were compared with the profiles from radiosondes in the period June 2016–October 2018 (~~Fig. 2~~ not shown). A slight cold bias is present (< 0.4 K). The RMSE increases with altitude, but in the lowest 2.5 km the RMSE is still below 1.8 K. For cloud top temperature, the temperature retrieved from the MWR elevation scan was linearly interpolated between the retrieval levels to cloud top height.

2.3 Circulation-weather-type

Since the local wind direction in the lower troposphere above Ny-Ålesund is heavily influenced by the orography (Maturilli and Kayser, 2011), the circulation-weather-type (CWT) based on Jenkinson and Collison (1977) was applied in order to evaluate cloud properties in the context of the regional wind field. Using 850 hPa geopotential height and shear vorticity from ERA-Interim, the flow at each time (0, 6, 12, and 18 UTC) was classified as either W, NW, N, NE, E, SE, S, SW, cyclonic, or anticyclonic. 16 grid points centered around Ny-Ålesund were used, so that the area covered is approximately 300 in meridional and 100 in zonal direction (77.5–80.5 N, 9.75–14.25 E, see Fig. 1). The approach aids in assessing whether the observed clouds were advected to the site from the open sea or over the island, and the proximity of high and low pressure systems.

3 Methods

3.1 Identification of persistent low-level mixed-phase clouds

To identify P-MPCs, each profile was evaluated individually to detect low pure-liquid and liquid-topped mixed-phase cloud layers, after which the persistency of the liquid layer was considered. Using Cloudnet target classification, the first step was to identify different cloud layers in each profile. Here a cloud layer refers to a continuous (gaps of <4 height bins, corresponding to 80 m, were omitted) layer of cloud droplets and/or ice. Each layer in the profile was classified as ice-only, liquid-only, or mixed-phase. To distinguish between low stratiform and deep multi-layered mixed-phase clouds, only profiles with a single liquid layer and the liquid layer being close to cloud top were considered. In practise, the detected upper boundary of the liquid layer was required to be in the uppermost 20 % of the cloud layer. The requirement for liquid being exactly at cloud top was relaxed since the ceilometer signal cannot necessarily penetrate the entire depth of the liquid layer. These criteria (single liquid layer, liquid close to cloud top) were very effective in selecting the desired low-level mixed-phase cloud regime. However, some mid-level clouds also fulfilled the criteria, and therefore we limited cloud top height to be below 2.5 km. For the remaining profiles, that all contain either liquid-only or liquid-topped mixed-phase clouds, the persistence of the liquid layer was evaluated. We only included clouds where the liquid layer existed for a minimum of one hour, with gaps ≤ 5 min. Since the focus of this study is on mixed-phase clouds, we further excluded clouds where no ice was detected. Note, that continuous presence of ice was not required, only the cloud liquid had to persist in time. The result is a data set with clouds below 2.5 km where liquid is located at cloud top and persists at least one hour, and at some point in time ice is associated with the liquid layer. Note, that time periods where another cloud layer is found above the P-MPC are not excluded. Figure 2 shows an example of the identified persistent MPC as well as ~~other~~ another mixed-phase ~~clouds~~ cloud. Despite the strict criteria, such clouds were present 23 % of the observational time.

In addition to identifying the time periods with P-MPCs present, the Cloudnet data was used to determine the base of the liquid layer and the cloud top height. A P-MPC case was defined as the time from the beginning to the end of the identified persistent liquid layer. Furthermore, we consider the layer from liquid base to cloud top as the cloud and everything below liquid base to be precipitation. This definition was chosen because the liquid base is well defined from the ceilometer observations.

Considering the focus on a persistent liquid layer identified by vertically pointing measurements, the cases included implicitly require either very low wind speeds, or a larger cloud field being advected over the site. When another cloud is detected above the P-MPC, the possibility that it contains undetected liquid cannot be excluded, and in these cases the measured LWP cannot be unambiguously attributed to the liquid layer of the P-MPC. ~~The presence of rain or drizzle in the column causes the same problem.~~ Hence, those time periods were flagged to be removed in any analysis of the cloud's liquid content. Unfortunately, we cannot make the assumption that upper cloud layers would not impact the liquid content of a P-MPC (Shupe et al., 2013). The presented LWP distributions are therefore only representative for single-layer cases. Furthermore, all columns with liquid precipitation or drizzle were excluded, leading to a loss of data mainly in the summer months. While this is somewhat unavoidable (e.g. when the MWR measurements suffer from a wet radome), it leads to the exclusion of rather warm precipitating P-MPCs from the analysis. [the last four sentences were moved here from Sect. 4.2]

3.2 Detecting surface coupling

3.2.1 Defining coupling with radiosonde profiles

The thermodynamic coupling of the P-MPC to the surface was determined based on the θ -profile. A quasi-constant profile was taken to indicate a well mixed layer, while an inversion denotes decoupling between different layers. For the sounding profiles, we simplified the methodology of Sotiropoulou et al. (2014). The cumulative mean of θ from the liquid layer base height downward is compared to θ at each level below the cloud. If this difference exceeds 0.5 K, the cloud is considered decoupled. Fig. 3 a and b show two example cases, one for a coupled and one for a decoupled cloud, respectively. Both profiles demonstrate a structure typical for stratiform Arctic MPC: a temperature inversion at cloud top, below which a well mixed layer is identifiable. In the case of the coupled P-MPC (Fig. 3a), the well-mixed layer extends to the surface. For the decoupled P-MPC (Fig. 3b) the well-mixed layer extends 200 m below the liquid layer base, below which several weaker temperature inversions and a generally stable stratification can be identified.

3.2.2 New continuous method

To continuously evaluate the coupling of the P-MPC to the surface, we developed a new method based on surface observations and the potential temperature profiles retrieved from the MWR, which are ~~available~~ available more frequently, i.e. every 15–20 min, compared to radiosonde data (Sect. 2.2.3). At each time when a MWR θ -profile was available, the cloud was classified as either coupled or decoupled based on a two step algorithm. First, the stability of the surface layer was evaluated using the measurements of the the meteorological station. The premise of this criteria is that if the surface layer is stably stratified, the cloud must be decoupled from the surface as there exists a stable layer between the surface and cloud base. The θ -profile is used as a proxy for stability. If the gradient of the 30 min mean θ between 2 and 10 m was positive (e.g. an inversion was present between 2 and 10 m), the surface layer was considered stably stratified, and therefore the cloud decoupled. If this was not the case, the second criteria based on the MWR θ -profile was used. We calculate the difference in potential temperature ($\Delta\theta$) between the surface level and at the height half way to the liquid base height. If $\Delta\theta$ is below the threshold of 0.5 K, the cloud

220 at this instance was considered coupled, and otherwise decoupled. The ~~temperature profile retrieval has limited ability to detect inversions layers, yet~~ reason for using the height equaling half of the liquid layer base height can be understood by comparing the θ -profiles from sounding and MWR in Fig. 3 a and b. While the general shape of the profile can be retrieved from the MWR measurements, it is not possible to resolve sharp inversions or detailed structures of the profile. Yet temperature inversions are very common at the top of MPCs P-MPCs. The comparison of MWR profiles with ~~soundings shows how all available soundings~~ when a P-MPC was present (Fig. 3c) shows that the accuracy of the retrieved θ -potential temperature is reduced in the vicinity of the liquid layer top (Fig. 3b). ~~It is for this reason that we estimated the temperature gradient in the subcloud layer using the retrieved θ at and that the influence extends to below the liquid layer base. At 0.5*liquid base height, as the RMSE at this height is still~~ the impact of cloud top inversion is smaller than at liquid base and the RMSE is below 1 K, which is why we chose this height to determine the stability of the subcloud layer. Note, that it should not be inferred that the method can only detect decoupling occurring in the lowest half of the subcloud layer. When decoupling occurs above the layer explicitly included, it is common that the lower half of the subcloud layer is at least partly stably stratified, as can also be seen in the example of Fig. 3b, prompting a correct decoupling classification.

As the final step, the individual profiles were considered together to define the degree of coupling of each observed P-MPC case. For each detected cloud event, the number of coupled and decoupled profiles were counted. If all profiles were decoupled, the P-MPC was considered fully decoupled. When more than 50 % of the profiles were found decoupled, the P-MPC was defined as predominantly decoupled. The rest were considered coupled.

3.2.3 Comparison of methods

The performance of the new method for estimating the coupling for each individual profile was evaluated using the soundings as a reference. We restricted the soundings to cases for which the cloud was present from the launch time until the sonde passed a height of 2.5 km (maximum cloud top height considered). Those soundings were compared to the MWR profile closest (but not more than 20 min away) to the radiosonde launch time. The sounding-based diagnosis found ~~33-31~~ % of the evaluated P-MPCs coupled and ~~67-69~~ % decoupled, compared to 18 % and 82 %, respectively, for the newly developed method for the corresponding clouds (Fig. 3d). This suggests a tendency in our method towards decoupling. However, the sounding profiles may miss very shallow surface based inversions. For ~~21-24~~ % of the profiles considered as coupled based on the radiosondes, the 2 and 10 m temperatures indicate a surface inversion. Classifying these clouds as decoupled instead changes the ratio of coupled and decoupled P-MPCs from the sounding data set to ~~26-23~~ % and ~~74-77~~ %, which is closer to that found with the new method. The main disadvantage of our method is that the temperature profiles retrieved from the MWR measurements do not provide a detailed profile, rather the general shape of the profile, and so the developed method occasionally fails. Furthermore, the 10 m layer considered for surface stability is rather shallow and intermittent coupling could occur regardless of the thermodynamic profile structure.

3.3 Local wind conditions in Kongsfjorden Circulation weather type

255 Since the local wind direction in the lower troposphere above Ny-Ålesund is heavily influenced by the orography (Maturilli and Kayser, 2011), the circulation weather type based on Jenkinson and Collinson (1977) was applied in order to evaluate cloud properties in the context of the regional wind field. Using 850 hPa geopotential height and shear vorticity from ERA-Interim, the flow at each time (0, 6, 12, and 18 UTC) was classified as either W, NW, N, NE, E, SE, S, SW, cyclonic, or anticyclonic. 16 grid points centered around Ny-Ålesund were used, so that the area covered is approximately 300 km in meridional and 100 km in zonal direction (77.5°–80.5° N, 9.75°–14.25° E, see Fig. 1a). The approach aids in assessing whether the observed clouds were advected to the site from the open sea or over the island, and the proximity of high and low pressure systems.

3.4 Local wind conditions

260 The channeling of the ~~surface-free-tropospheric~~ wind along the fjord axis is a typical feature of an Arctic fjord (Esau and Repina, 2012, and 2013). Previous work has found the feature prominent also at Kongsfjorden (Maturilli and Kayser, 2017). It is well documented that despite the dominating westerly free-tropospheric wind direction, in Kongsfjorden the near surface wind tends to blow south-easterly along the fjord axis (Maturilli and Kayser, 2017; Beine et al., 2001) (Maturilli and Kayser, 2017; Beine et al., 2001; Jocher et al., 2012). This is usually attributed to katabatic forcing of the Kongsvegen glacier about 15 km east-southeast from Ny-Ålesund (Fig. 1), although Esau and Repina (2012) argued that for typical synoptic conditions the land-sea breeze circulation would be the dominant driver. The secondary mode in surface wind is from northwest, from the sea towards the island's interior. According to Jocher et al. (2012) the northwesterly surface winds are associated to cold air advection that relate to passing low-pressure systems. Beine et al. (2001) find this wind direction to be pronounced in June and July, which they associate with sea breeze and the melting of sea ice. In addition, at Ny-Ålesund ~~katabatic flow down the glaciers located south of the village are observed. Also the southeasterly surface wind is at times associated with glacier outflows.~~ weak southwesterly surface winds are observed, caused by katabatic flow from the Zeppelin mountain range and the Broggerbreen glacier south of Ny-Ålesund (Jocher et al., 2012; Beine et al., 2001) under specific synoptic conditions (Jocher et al., 2012; Argentini et al., 2003). The local wind conditions impact the stratification of the local boundary layer (Argentini et al., 2003; Svendsen et al., 2002). Argentini et al. show that during the ARTIST campaign (15 March – 16 April 1998 at Ny-Ålesund) stable conditions were mainly observed with southeast wind and hardly ever with northwest wind. Unstable conditions occurred from 90° to 270° and under light wind conditions. Furthermore, large wind shear was observed to generate turbulence and lead to neutral stratification. This brief summary of previous studies demonstrates the complexities of the local wind conditions present at the AWIPEV station.

270 We cannot properly describe the circulation in Kongsfjorden from our point measurements at Ny-Ålesund or evaluate the drivers behind the local wind, nor are these processes within the scope of our study. However, it is possible that certain wind patterns are associated with ~~lifting air (for example forced by mountains or related to sea-breeze), increased shear (result of wind direction changing rapidly with altitude) that may enhance turbulence, or colder and drier air flowing in the surface layer below the cloud (outflow from glaciers).~~ All of these have the potential to phenomena (shear induced turbulence, drainage flows from mountains and glaciers transporting cold air into the sub-cloud layer) that modify the P-MPC studied.

285 To evaluate whether the local wind patterns modify the P-MPC, we identified the main modes in the 10 m wind direction and combined them with the circulation weather type to create a proxy for different wind regimes. ~~From the surface wind As~~

expected, three modes can be identified in the surface wind (Fig. 4a). The dominating wind direction (85° – 165°) corresponds to the direction out of the fjord to the open sea. Less pronounced but clearly identifiable are the two other modes that indicate flow from the sea into the fjord (270° – 345°) and the katabatic flow from the glaciers ~~located south of Ny-Ålesund south of the station~~ (200° – 270°). ~~Surface wind from southwest was commonly observed only when low synoptic wind speed allowed the local katabatic flow to establish~~ Wind speed above 12 ms^{-1} was only observed between 90° and 120° . Seasonal wind roses are provided in Appendix A2. The frequency with which each surface wind mode was associated with the different weather types during the cloud observation period (June 2016 to October 2018) is illustrated in Fig. 4b. For most circulation weather types, the southeasterly surface wind dominated and the northwesterly was rare. An exception were the weather types N and NW, for which the northwesterly direction was most common.

To illustrate how the weather type and surface wind direction modes correspond to different wind profiles, the average wind direction profiles based on radiosonde data from ~~September 2011–June 2016~~ to October 2018 are shown for weather type W and N (Fig. 5). ~~A longer time period is included here to increase the number of soundings available for each wind regime. For weather type W when 4c). When~~ the surface wind direction was northwesterly, the average direction changed only slightly from the 280° in the free troposphere to align with the fjord axis at about 310° . The largest variation in the lowest 200 m was exhibited by the southwesterly surface wind direction, ~~and wind speeds close to the surface were very low, typically below 4 (Fig. 4a).~~ The most common regime (surface wind from southeast) had an average profile with free-tropospheric wind from the west, turning south and all the way to the southeast (120°) in the lowest 300 m. ~~It was also associated with the highest surface wind speeds (Fig. 4a). For weather type N, the southeasterly surface wind is associated with a profile where the wind turns in the opposite direction: further east and then north from the surface upwards. When the surface wind is from southwest, the wind turns rapidly (on average in the lowest 400) to north. The northwest surface wind is associated with the least change for weather type N in wind direction with altitude, as the wind only slightly turns when channelled along the fjord. The average profiles suggest that winds align with surface wind direction in a layer 10–500 above the surface, and above this is a layer 200–500 deep where the wind turns to the free-tropospheric wind direction. Furthermore, the circulation weather type gives a good indication of the wind direction in the free troposphere. Comparing Figures 5a and 5b Figure 4c illustrates why a~~ combination of surface and free tropospheric wind direction is needed to isolate different patterns. Considering the moderate standard deviation in the wind direction profiles shown in Fig. 5 4c, it is reasonable to assume that each surface wind direction mode together with the weather type, which describes the mean regional wind direction at 850 hPa, describes a certain wind pattern, and thus gives a first estimate of the wind conditions around Ny-Ålesund.

3.5 Statistical tools

To test the statistical significance of differences between two or more distributions, the Mood's median test to compare the medians in different populations was used (Sheskin, 2000). This test was chosen because it does not require normally distributed data and the compared samples can be of different sizes. The median of each population is compared to the median of the distribution including all data, and the Pearson's χ^2 test is used to test the null hypothesis that medians from different

populations are identical. To reject the null hypothesis thus leads to the conclusion that the different populations have different medians.

The data points in the time series of the variables tested (LWP, IWP, cloud top temperature, and cloud base height) are correlated with each other, and can not as such be used in the statistical test. We assume that each P-MPC case is independent of each other, and for cloud top temperature and cloud base height use the medians for each case for testing. LWP and IWP were found to vary more within each case, and therefore several data points from every P-MPC case were sampled. For this, we estimated the de-correlation time scale as the time where the auto-correlation function, computed for each P-MPC case individually, reaches zero. For the majority of P-MPC cases there were too many gaps in the data to reliably compute the auto-correlation function, and hence no de-correlation time scale could be estimated. From the values available, the median was calculated and then double the median was used as the de-correlation time scale Δt_{dcr} for all cases. For testing, the data was sampled randomly, with a minimum gap of Δt_{dcr} between the sampled data points.

4 Results and discussion

4.1 Occurrence of persistent MPC and other clouds

We first examine the frequency of occurrence of different types of clouds in the observation period of the cloud radar (~~10.6.2016–8.10.2018~~ 10 June 2016–8 October 2018) considering the 30 s averaged columns of the Cloudnet product. A cloud was found above Ny-Ålesund 76 % of the time measurements were running. The month-to-month variation was considerable, varying from 40 % to over 90 % (Fig. 5). Averaging for all years, cloudiness was slightly higher in summer (June–August; 80 %) and autumn (September–October; 77 %), and lower in spring (March–May; 69 %) and winter (December–February; 74 %). Intra-annual variation is pronounced in autumn, when cloud occurrence frequency varied from 69 % to 84 %. MPCs (defined here as any profile where co-located cloud liquid and ice are found) were present 41 % of the time, with a somewhat higher frequency in autumn. Liquid-only clouds (profiles with cloud droplets without co-located ice) had an overall occurrence frequency of 14 % and a clear seasonal cycle with most liquid-only clouds occurring in summer, and hardly any in winter or spring. Thus, the radiatively important cloud liquid was more often found in mixed-phase clouds, although the contribution of liquid-only clouds was significant-notable in summer. All of the presented figures are given relative to the amount of data available. The top panel of Fig. 5 shows the high data coverage obtained, implying that - with the exception of the first and last month - we can give a reliable estimate of the frequency of cloud occurrence within the detection limits of the instruments.

The persistent low-level mixed-phase clouds (P-MPC, see Sect. 3.1 for definition) cover 23 % of the data set, highlighting the relevance of this cloud regime. In total 1412 cases of P-MPC were identified. The 'all MPC' and the P-MPC occurrences in Fig. 5 are not directly comparable, since the first one refers to individual profiles and the latter is to a large extent defined by a temporally continuous liquid layer and also includes profiles without a mixed-phase layer detected. P-MPC were most common in summer (32 %) and occurred less often in winter (15 %) and spring (16 %), with autumn being the intermediate season (24 %). The P-MPC occurrence thus follows the seasonal cycle of cloud liquid occurrence (Nomokonova et al., 2019b).

For defining the persistence of the liquid layer some thresholds needed to be set, including how long gaps were allowed, and the minimum duration required. The choices made (5 min and 1 h) were motivated by the aim for a certain cloud regime, namely a stratiform mixed-phase cloud in the boundary layer. A sensitivity test allowing only 2 min gaps in the liquid layer showed the only major difference being in the occurrence frequency of P-MPCs, while the properties of the clouds or the seasonal cycle of P-MPC occurrence did not differ substantially.

4.2 P-MPC properties and regional wind direction

Figure 6 shows the occurrence of each weather type (used to determine the regional free-tropospheric wind direction, see Sect. 3.3) in our period of study, and the fraction of those times when a P-MPC was identified. In general, NE, SE and NW were less common than the other wind directions. For a given weather type, the fraction of P-MPC occurrence varied considerably. Almost a third of the time when winds were from west (W), a P-MPC was found at Ny-Ålesund. Weather types S, SW, NW, and anticyclonic were also favourable for P-MPC. Based on an evaluation of sounding profiles, the most common free-tropospheric wind direction for weather type anticyclonic was west (not shown). On the other hand, winds from north and east (weather types N, NE, and E) were less often bringing P-MPCs to the site. ~~This is likely a result of more humid air masses coming from the south (lower latitudes) and west (sea).~~ The weather types which are most commonly associated with P-MPCs can be determined by combining the occurrence frequency of each weather type and its P-MPC fraction (Fig. 6). Consequently, P-MPC were most often associated with the weather types W, SW, and anticyclonic, which include almost half (48 %) of all profiles.

The distributions of liquid layer base height, LWP and IWP and their dependence on wind direction are presented in Fig. 8. The base of the liquid layer was usually between 540–1020 m above the surface, with mean and median liquid base height of 860 and 760 m, respectively. The typical P-MPC thus lies above the fjord at a height fairly close to the mountain tops. Fewer P-MPC were associated with weather types NE, E and SE, and with mean liquid base heights well above 1 km these were found at larger altitudes than most of the P-MPC. The mean LWP for P-MPCs was 35 gm^{-2} with a standard deviation of 45 gm^{-2} . On average most liquid was found in the P-MPC in weather type SW (49 gm^{-2}), and least in weather type NE (12 gm^{-2}). However, the variability within each weather type was larger than the differences between the weather types. The IWP distributions are strongly skewed (Fig. 8e 7c) towards low values. Zeros were ignored, but all non-zero values were included. For all P-MPCs, the mean and median IWP were 12 and 2.1 gm^{-2} , respectively. Between the different weather types, the mean (median) varied from the $5.6 (1.1) \text{ gm}^{-2}$ of weather type SE to the $17 (6.2) \text{ gm}^{-2}$ of weather type NW. The weather types NW, W and SW stand out in terms of high IWP, and have a mean IWP of 16 gm^{-2} . Overall, the westerly weather types (SW, W and NW) were associated with lower P-MPCs and with more liquid and ice (mean LWP 42 gm^{-2}), while the easterly weather types (SE, E and NE) were less common, distinctly higher and connected to the lowest average LWP and IWP.

~~Our ability to estimate the amounts of liquid and ice in the P-MPCs is restricted by the accuracy of the retrievals, as well as the conditional sampling that needs to be applied. We excluded all times when liquid precipitation was found in the column, leading to a loss of data mainly in the summer months. Fortunately, this is the time with most abundant P-MPCs. While this is somewhat unavoidable (e.g. when the MWR measurements suffer from a wet radome), it leads to the exclusion of rather warm~~

385 precipitating P-MPCs. For the LWP distributions presented, only profiles where no other cloud was found above the P-MPC were included (Sect. 3.1). Unfortunately, we cannot make the assumption that upper cloud layers would not impact the liquid content of a P-MPC (Shupe et al., 2013). The presented LWP distributions are therefore only representative for single-layer cases.

Large scale advection and air mass properties are known to influence MPC properties (Mioche et al., 2017; Qiu et al., 2018, amongst others). Previous studies suggest that at Svalbard northerly flow is often associated with cold air masses originating from the central Arctic, and that southerly flows bring warmer and more humid air from lower latitudes (Dahlke and Maturilli, 2017; Knudsen et al., 2018; Kim et al., 2017; Mioche et al., 2017). Accordingly, we find a higher P-MPC occurrence with winds from south than from north (24 % and 14 % of the time with weather types S and N, respectively; Fig. 6). Most P-MPC were observed below Furthermore, the open sea west of the Svalbard archipelago might act as a local source of humidity and heat. Here we use temperature at 1.5 km (corresponding to the 850 hPa level, and therefore the weather type should be interpreted as a general wind direction above the boundary layer, rather than the actual advection direction of) and integrated water vapor (IWV) from the MWR to represent the atmospheric temperature and humidity conditions under which the P-MPC were occurring. However, the were occurring. In agreement with previous studies, Fig. 8 shows that the highest average IWV and warmest temperatures were associated with southerly winds, while the lowest average IWV and coldest temperatures with northerly winds. The domain considered for the weather type (Fig. 1a) is too small to describe large scale advection or air mass origin, and these effects are superimposed with the influences the Svalbard archipelago has on the clouds. Additionally, temperature and humidity, which are key air mass characteristics for cloud processes, vary seasonally (Nomokonova et al., 2019b; Maturilli and Kayser, 2017). To evaluate the connection between but Fig. 8 suggests the weather type is nonetheless a useful proxy for air mass properties. The average IWV and 1.5 km temperature can explain the first order variation in P-MPC occurrence and LWP between weather types. The south-southwesterly winds are warm and humid, and different air masses would therefore require a more detailed analysis utilizing back trajectories and characterization of air mass properties. Nonetheless, the combination of the presumed effects of large scale advection and the influence of the island provide an explanation for the characteristics presented in Figures 6 and 8: Southwesterly and westerly free-tropospheric winds were associated with most are associated with frequent occurrence of P-MPC and the highest average LWP and IWP (more humidity available from lower latitudes and from the sea), while the southeasterly to northeasterly wind cases have the least P-MPC, and comprise the lowest average LWP with relatively high amounts of liquid, compared to the north-northeasterly winds, which are drier and colder, and are associated with less frequent P-MPC occurrence and lower LWP (Fig. 6, 7b, and 8a). Owing to the complexity of ice micro-physical processes, such direct relationship cannot be found between atmospheric humidity and temperature (Fig. 8) and IWP (drier air masses from north and less humidity available over land) Fig. 7c). On the other hand, as already noted above, Fig. 7 shows a clear contrast between the properties of easterly and westerly P-MPC. These differences cannot be explained by the IWV and 1.5 km temperature distributions, which are rather similar for weather types W and E. Hence, atmospheric temperature and humidity are important, but not the only relevant forcing for P-MPC at Ny-Ålesund.

The influence of the island and its orography clearly affects the height of the liquid layer (Fig. 8a). The moisture available from the sea is likely contributing to the higher total water paths for weather types SW, W and NW (Fig. 8). 7a). The median

420 altitude of the P-MPC base with easterly winds (weather types NE, E and SE) was above the height of the mountain tops, suggesting that the clouds usually were advected to the site above the mountains rather than forming locally in the fjord. The P-MPC associated with easterly winds were also less frequent (Figures 6 and 8a7a). If we assume the majority of observed P-MPC being of advective nature, the low occurrence frequency with winds from east would imply less cloud formation over the island compared to over the sea, or dissipation of cloud fields while being advected over the island. Mioche et al. (2015) found
425 less low (below 3 km) MPC over land than over sea in the Svalbard region in spring and winter, while in summer and autumn the differences were small. Cesana et al. (2012) studied liquid containing clouds in the Arctic, and found less low (below 3.36 km) liquid containing clouds above Svalbard than over the surrounding sea in all seasons. Although direct comparison is not possible due to inconsistencies in the observation techniques, cloud sampling and the considered area, the mentioned studies all indicate that the ~~Svalbard archipelago has an influence on~~ influence of the Svalbard archipelago is to decrease the amount
430 of low liquid bearing clouds.

The combination of the effects of large scale advection and air mass properties, as well as the influence of the Svalbard archipelago, can provide an explanation for the dependence of the P-MPC properties on weather type presented in Fig. 6 and 7. Southwesterly and westerly free-tropospheric winds were associated with most P-MPC and the highest average LWP and IWP, likely due to higher amounts of humidity available from lower latitudes. The southeasterly to northeasterly winds had the
435 least P-MPC, and comprise the lowest average LWP and IWP, related to the drier air masses from north and less favourable conditions for cloud formation over the island. Other mechanisms can be considered to further explain the observed IWP variation. Ice formation could be enhanced in the cold temperatures for weather types N and NE (Fig. 8), whereas the higher IWP for weather types SW, W and NW might be related to larger amounts of super-cooled liquid available in the P-MPCs (Fig. 7b,c) or higher aerosol concentration in airmasses advected from lower latitudes.

440 4.3 Seasonality

The seasonal variation of the studied P-MPC properties and atmospheric conditions at Ny-Ålesund are presented in Fig. 9. In agreement with previous studies (Nomokonova et al., 2019b; Maturilli and Kayser, 2017), the highest average temperature and humidity are found in summer, and the lowest in winter and spring (Fig. 9a,b). The height of the P-MPC shows a clear seasonality, with lower liquid base height in summer and higher in winter (Fig. 9c). Zhao and Wang (2010) evaluated five
445 years of low-level MPC occurrence and properties clouds (cloud base below 2 km) observed at Utqiagvik (previously known as Barrow), Alaska, and also found a seasonality in cloud height with a minimum in summer. Furthermore, these results are in agreement with the seasonality in cloud height at Ny-Ålesund reported by Shupe et al. (2011). The IWP distributions show a clear seasonality, with low values in summer and autumn and a clear maxima in spring (Fig. 9e). The low IWP in summer and autumn (median 0.2 and 1.0 gm^{-2} , respectively) can be attributed to relatively warm temperatures close to 0°C. The median
450 IWP in spring (7.5 gm^{-2}) is almost 2-fold of the median IWP in the winter (4.0 gm^{-2}), which can hardly be attributed to the different temperature conditions (Fig. 9b). The higher IWP in spring compared to winter (Fig. 9a), however, can play a role. Furthermore, the high IWP in spring could be related to the generally higher aerosol loading in the Arctic atmosphere in the late winter and spring, a time period also known as the Arctic haze season (Quinn et al., 2007).

455 ~~Finally, we~~ On the contrary, the LWP distributions show a minimal seasonality despite the seasonal variation of IWV and
1.5 km temperature related to the P-MPC (Fig. 9a,b,d). The highest (lowest) median LWP in summer and spring (winter) was
24 gm^{-2} (18 gm^{-2}), and the seasonal mean values varied from 33 to 36 gm^{-2} . Note, that this result does not imply a lack of
seasonal variability in overall cloud LWP (see Fig. 5 in Nomokonova et al., 2019a), only in the specific cloud regime evaluated.
One challenge of the algorithm to identify the P-MPC are thick liquid layers where Cloudnet only identifies the lowest parts
of the layer as containing liquid. The problem was partly mitigated by relaxing the criteria for liquid presence at cloud top,
460 nonetheless we find cases with a thick liquid layer that do not fulfill the criteria of liquid topped mixed-phase layer and the rest
of the cloud gets cut off (see Fig. 2 at 12:00 on 30 May 2018). This artificially limits our data set to clouds where the liquid
layer is thin enough, and there might be some clouds with more liquid that are not included in our analysis. Considering the
LWP distributions were skewed towards lower values (Fig. 7b), these cases are likely to be a minority for the cloud regime
considered. However, it is possible that the average LWP is somewhat underestimated. In addition, it could be that the cloud
465 detection algorithm limits the considered cases to a specific LWP regime, which results to the lack of seasonality in the LWP
of the P-MPC.

Since P-MPC properties (excluding LWP) as well as atmospheric temperature and humidity vary seasonally, a seasonal
dependency in wind direction could explain the weather type dependent variations in P-MPC properties found in Sect. 4.2.
To examine this possibility, Fig. 10 shows the proportion of P-MPC observations in each season for every weather type. The
470 observation period of 2.5 years from June 2016 to October 2018 together with the seasonal variation in P-MPC occurrence
(Fig. 5) lead to the uneven distribution of data between seasons. Overall, the summer months contribute most to the data set.
However, there are no extensive differences found between the weather types. Most noteworthy is the high spring and low
autumn occurrence of NW, which might contribute to the high IWP for this weather type (Fig. 7c). Furthermore, N and E were
relatively more common in winter, N and SE more common in spring, and N less common in autumn. Given the lack of a
475 distinct signal, we believe the seasonal variation in wind direction plays a minor role in the weather type dependent differences
in P-MPC occurrence and properties described in the previous section.

We further compare properties of the P-MPC at Ny-Ålesund ~~and their seasonal variation~~ to observations of similar cloud
regimes at other Arctic sites. Only studies that comprise at least one year of observations were considered ~~to ensure the results~~
~~are somewhat comparable~~. Shupe et al. (2006) evaluated MPCs observed at the one year long Surface Heat Budget of the Arctic
480 Ocean (SHEBA) campaign, and found an annual average LWP and IWP of 61 gm^{-2} and 42 gm^{-2} , respectively. ~~Both IWP and~~
~~LWP were found to have a maximum in late summer and autumn~~. The study did not explicitly focus on low-level clouds, but
found that 90 % of the observed MPC had cloud base below 2 km. De Boer et al. (2009) focused on single-layer mixed-phase
stratus at Eureka, Canada, and reported seasonal mean LWP to vary between 10 and 50 gm^{-2} . Zhao and Wang (2010) ~~evaluated~~
~~five years of low-level clouds (cloud base below 2) observed at Utqiagvik (previously known as Barrow), Alaska, and~~ show
485 monthly mean values for LWP ~~at Utqiagvik~~ to vary from 10 to 100 gm^{-2} , and ~~for IWP from~~ 10 to 25 gm^{-2} ~~for IWP~~. Similarly
to SHEBA, at both Eureka and Utqiagvik the maximum LWP was found in autumn. However, at Eureka as well as Utqiagvik
a maxima in the amount of ice in MPCs was found in spring as well as autumn. The differences in seasonal cycles of LWP
and IWP at different sites could be due to different forcing conditions, in addition to the choice of the cloud regime that might

also play a role. Sedlar et al. (2012) included all single-layer clouds below 3 km and found that most of the LWP distribution was within 0 to 100 gm^{-2} , with slightly higher values in the data set from SHEBA than Utqiagvik. ~~These~~ The average figures are comparable to those observed for P-MPC at Ny-Ålesund, although the mean values in our study are at the lower end of the range reported at Utqiagvik and SHEBA ~~using different cloud sampling.~~

~~We found P-MPC to occur in all seasons, however, in summer more frequently than the rest of~~ Finally, the year. ~~Shupe et al. (2011) season~~ variation of P-MPC occurrence is compared with previous studies in the Svalbard region. Shupe et al. (2011) as well as ~~Maturilli and Ebell (2018)~~ report most clouds in summer and early autumn above Ny-Ålesund, agreeing with our findings. ~~Furthermore, the observed seasonality in cloud height with minimum in summer (Fig. 11e) has also previously been found at Ny-Ålesund (Shupe et al., 2011) as well as at Utqiagvik (Zhao and Wang, 2010).~~ On the contrary, Mioche et al. (2015) identified most low-level (below 3 km) MPC in the Svalbard region in autumn and a minimum in occurrence in summer based on the synergy of the measurements from CLOUDSAT and CALIPSO. ~~Due to the fact that~~ P-MPC commonly contain very low amounts of ice ~~was present in the P-MPC~~ which might be below the sensitivity limit of the satellite observations ~~could explain this explaining some of the~~ disagreement. Furthermore, Mioche et al. (2015) were missing clouds below ~~clouds below 500 meters~~ m due to the blind-zone of CLOUDSAT, and since clouds generally are lower in summer this would lead to a higher fraction of missed clouds in this season. In any case, considering the large month to month variation in cloud occurrence (also shown by Shupe et al., 2011), different results when considering different time periods can be expected. Our time series might still not be long enough to give a precise estimate of the seasonal variation of cloud occurrence frequency.

4.4 Surface coupling

Figure 11a shows the fraction of observed P-MPC classified as coupled, predominantly decoupled and fully decoupled in each season. 63 % of all observed P-MPC cases were found fully decoupled, and only 15 % were coupled. The degree of coupling had a clear seasonal cycle, with decoupling being the dominant mode in autumn and winter, and most coupled P-MPCs occurring in summer. The observed seasonality in the surface coupling of P-MPC could be related to the overall higher lower-tropospheric stability in winter, which could limit the coupling of the cloud. Previous studies have found that the coupling of low Arctic MPCs depends on the proximity of the cloud to the surface since the cloud driven mixing layer is more likely to reach the surface if the cloud is low (Shupe et al., 2013; Brooks et al., 2017). Also in our data set the median cloud base height for decoupled P-MPCs (1010 m) is ~~almost double of~~ considerably larger than the median cloud base height of the coupled P-MPCs (620 m, ~~see~~) (Fig. 11b). For P-MPC with liquid base heights of more than 1.5 km coupling to the surface was not observed. ~~Additionally,~~ P-MPC were on average higher in winter and lower in summer (Fig. 9c), which could partly explain the seasonal variation in the frequency of surface coupling. ~~We also find that surface wind direction is related to coupling. Coupling was most common with northwest surface wind (from the sea) and least common with the southeast surface wind (towards the sea), and the same behaviour was found for every season (not shown).~~

To evaluate the effect the surface coupling has on cloud properties, we only considered P-MPC in weather types SW and W in order to limit the different factors in play. These clouds include the full range of coupling states, and cover one third of the data set (Fig. 8a 7a). The coupled P-MPC had more liquid than the fully and predominantly decoupled P-MPC (Fig. 12a). The median

LWP did not differ significantly between the predominantly and fully decoupled P-MPC (25 and 28 gm^{-2} , respectively), while the median LWP for coupled cases was clearly larger (47 gm^{-2}). Differences in IWP between the coupling states were small (Fig. 12b). The medians did not vary notably (~~from 10 to 13~~ significantly (from 11 to 12 gm^{-2}), but the larger IWP values (between 30 and 100 gm^{-2}) were less likely for the coupled P-MPC. From the LWP and IWP distributions it follows that the total amount of condensed water (~~total water path~~ = LWP+IWP) was higher for coupled than predominantly or fully decoupled P-MPC. This suggests either a source of humidity from the surface that is not available for the decoupled P-MPC, or a smaller sink.

Many ice micro-physical processes have a temperature dependency (Lamb and Verlinde, 2011), and the observed differences in LWP and IWP distributions between coupled and decoupled P-MPCs could be caused by different sampling across the temperature range. Observed cloud top temperatures ranged from -28 to $+5^\circ\text{C}$, with most P-MPC occurring at the warm end of this range (Fig. 12c). As the persistent liquid layer is the defining feature of the P-MPC, it is not surprising that they occurred more often at warmer temperatures where liquid is generally more abundant. The coldest P-MPC (cloud top temperatures below -18°C) were always decoupled, and were occurring in winter and early spring. The cloud top temperature distributions were very similar for the coupled and predominantly decoupled P-MPC, suggesting that the differences in IWP and LWP distributions between these two groups can not be explained by a varying frequency of different temperature regimes. The cloud top temperature distribution of fully decoupled P-MPC differs from that of the predominantly decoupled and coupled clouds by having larger number of cold cloud tops and a smaller peak at the warm end of the distribution. Yet the IWP and LWP distributions do not differ substantially between fully and predominantly decoupled P-MPC. Although the observed differences in LWP and IWP between coupled and fully decoupled P-MPC could be caused by differences in temperature, we cannot explain the differences between predominantly decoupled and coupled, or the similarity of the predominantly and fully decoupled P-MPC simply from the cloud top temperature distributions.

The analysis presented only included weather types SW and W. These weather types are amongst the weather types having largest average LWP and IWP. The variation in LWP and IWP between coupled and decoupled P-MPC for the other weather types would therefore be smaller in absolute numbers. Including all weather types, the medians for LWP for coupled, predominantly and fully decoupled were 34, 22 and 20 gm^{-2} , and the medians for IWP 7.5, 9.4 and 9.4 gm^{-2} , respectively. The outcome that coupled P-MPC had more liquid, and that differences in median IWP were small, is the same. One needs to keep in mind that these numbers are dominated by the westerly weather types which cover the bulk of the data. It is possible that different relationships between cloud properties of coupled and decoupled clouds would be found for weather types which have distinctly different mean wind conditions. While we cannot conclude that the presented results hold for all situations occurring at Ny-Ålesund, they describe the most common conditions.

The comparison between the coupling detection from sounding and the new method based on MWR and surface observations implied that the new method is more inclined to consider a profile decoupled (Sect. 3.2.3). Yet, the similarity of the LWP and IWP distributions for predominantly and fully decoupled P-MPC suggest that these groups were very similar. Considering cloud properties, it does not seem that the predominantly decoupled would be mistakenly considered more decoupled than they are. It is possible that our method erroneously classifies weakly coupled P-MPC as predominantly decoupled, and that in these

cases the interaction with the surface is limited and does not modify the cloud properties considerably leading to similar LWP and IWP distributions for these clouds and the actually decoupled P-MPC. Accordingly, we conclude that decoupling might be overestimated, but this does not have serious consequences on the results on cloud properties. Considering the different estimates (Fig. 2e 3d and 11a), we can regard 63–82 % of the P-MPC decoupled, and 15–33 % coupled. Moreover, intermittent turbulence and the coupling it may lead to are rather challenging for our approach, as the thermodynamic profile takes time to adjust. However, the turbulent transport of heat can be assumed to be similar as the transport of any other scalar. If the turbulence that occurred was too short-lived to modify the temperature profile distinctly, it would also be unlikely to transport great amounts of water vapor or aerosols to the cloud layer.

Shupe et al. (2013), Sotiropoulou et al. (2014) and Brooks et al. (2017) have evaluated the coupling of low clouds during the ASCOS campaign (August–September 2008) using different methods and slightly different time periods, and observed decoupling from surface 75 %, 72 % and 76 % of the time, respectively. Their measurements were mostly of clouds above sea ice, and for a shorter time period. The results are therefore not directly comparable with the multi-year statistic presented here. Moreover, the mechanisms that lead to decoupling at ASCOS were likely different than at Ny-Ålesund. Like Shupe et al. (2013), but unlike Sotiropoulou et al. (2014), we found a difference in LWP between coupled and decoupled clouds (Fig. 12a). If we assume that the (sea) surface can provide a source of moisture for the P-MPC, coupling could add moisture to the cloud layer and lead to a higher total water path. Considering the small differences in IWP (Fig. 12b), it does not seem that the surface would be an important source for INP, or there are some other mechanisms that limit ice formation in coupled clouds where more liquid water is present. The observed seasonality in the surface coupling of P-MPC (Fig. 11a) could be related to the overall higher lower-tropospheric stability in winter, which could limit the coupling of the cloud, as well as to the lower cloud base height in summer (Fig. 11c) that makes it easier for the cloud to couple to the surface due to its proximity.

4.5 Local wind patterns around Ny-Ålesund

The effects local wind winds have on the P-MPC were evaluated using the weather type together with the surface wind direction as a proxy for the wind conditions at Ny-Ålesund (Sect. 3.4). The most common wind situation for the P-MPC at Ny-Ålesund is a southeasterly surface wind underlying westerly/southwesterly upper winds (Fig. 4, 6). Hence, the wind turns from the surface upwards to the almost opposing direction by 1.5 km height (Fig. 5a). ~~With almost all free-tropospheric wind directions the most common surface wind is from southeast (Fig. 4), indicating a local driver that acts in nearly all synoptic conditions.~~ Directional wind shear is therefore commonplace for P-MPC at Ny-Ålesund (Fig. 4b), either in or below the cloud layer. The magnitude of the wind direction change varies with the free-tropospheric wind. The only exception are weather types N and NW, for which the most common surface wind is northwesterly, and the wind does not turn, or only turns slightly, with increasing altitude. A further consideration related to near the surface wind direction is the history of the boundary layer. The air has experienced very different surface properties when moving from open sea to land with northwesterly near surface wind surface wind or from mountainous, often snow and ice covered terrain terrain, to a flat sea surface with southeasterly near surface wind.

Fig. 9 The influence of local winds on the P-MPC was found to be limited. Figure 13a shows the fraction of time with P-MPC occurring (similarly to Fig. 6) for each weather type and surface wind direction combination. Weather types cyclonic and anticyclonic are somewhat hard to interpret, as these are associated with varying free tropospheric wind directions above the site, and were therefore not included. The low number of cases with southwest and northwest surface wind limits the possibilities to compare different surface wind regimes for most of the weather types. For weather types SW and W the southwest surface wind was associated with higher frequency of cloud occurrence (~~32 % and 35 % of the time a P-MPC was present for SW and W, respectively~~) compared to the southeast surface wind (~~25 % and 31 % for SW and W~~), and in the case of weather type W also compared to the northwest surface wind (~~31 %~~). In contrast, for weather type N northwest surface wind had P-MPCs most often (~~18 %~~) and southwest the least (~~11 %~~). Based on this analysis no overall tendency for certain surface wind direction, or the amount of directional shear between the surface and the free-tropospheric wind, to increase or decrease P-MPC occurrence was found.

~~The cloud properties associated with different surface wind directions were compared separately for each weather type. Only Regarding P-MPC properties, no strong relationships with surface wind direction were identified. Only the main findings are summarized here and further details are provided in Appendix A1. Considering weather types N, W and SW were considered in order to have a sufficient amount of data (at least 30 cases) in each group being compared (Fig. A1). The, which have the most cases across different surface wind directions, no statistically significant differences were found in the median liquid base height did not differ significantly (on a 95 % confidence level) for any of the three weather types evaluated or cloud top temperature.~~ The northwest surface wind was associated with the highest ~~average LWP~~, however, for weather type SW the differences were not statistically significant. For weather type N the median LWP for northwest surface wind was 22 gm^{-2} compared to the ~~the~~ 12 and 7.8 gm^{-2} of southeast and southwest surface winds. Also for weather type W the northwest median LWP, possibly due to higher level of humidity available over the open sea. The southwest surface wind was associated with highest median LWP (39 gm^{-2}), however the lowest median LWP was with southeast surface wind (18 gm^{-2}). The median IWP varied insignificantly (from 7.8 to 9.7 gm^{-2}) for weather type N. For weather type SW, the southwest surface wind had the highest median IWP at 18 gm^{-2} , almost double of the median of southeast (10 gm^{-2}) and northwest (9.1 gm^{-2}) surface winds. Similarly for weather type W the median IWP for southwest was a significantly higher IWP for weather types W and SW (median IWP 16 gm^{-2} , and only 11 and 9.6 and 18 gm^{-2} for southeast and northwest surface winds. Because of the temperature dependence of many micro-physical processes, it would be possible that the observed differences were a result of different temperature regimes dominating in the compared groups. However, no statistically significant difference in the cloud top temperature distributions were found (Fig. 10d).

One challenge of the phase detection is the temperature dependence of ice identification, and the accuracy of the thermodynamical data (from NWP) available for the Cloudnet algorithm. Many of the identified P-MPC are rather warm with temperatures close to zero (Fig. 10d). It is possible that some mixed-phase clouds were omitted due to missed ice, or that drizzle in slightly super-cooled liquid layers have mistakenly been identified as ice leading to false identification or overestimated ice water content. It is difficult to estimate how common these problems are., respectively). However, these clouds most likely have very

625 ~~low ice water content because of the proximity of the temperature to 0, and the impact on the presented results by over- or underestimated IWP is most likely minimal~~ variations in LWP and IWP were not found for all three weather types analyzed.

Local winds in Kongsfjorden were quite apparently connected to the coupling of the P-MPC (Fig. ~~11b~~ 13b). Coupling was most common with northwest surface wind (from the sea) and least common with the southeast surface wind (towards the sea), and the same behaviour was found for every season despite the seasonality of both surface wind direction and cloud coupling (see Appendix A2). For the P-MPC to be ~~thermo-dynamically~~ thermodynamically decoupled from the surface, a ~~layer of stable stratification~~ stably stratified layer needs to exist between the surface and the cloud base. Argentini et al. report a dependence of surface layer stratification on wind direction (Argentini et al., 2003, Fig. 5). Stable conditions were most often found with southeast surface wind, for which only 8% of the P-MPC were considered coupled. On the other hand, stable conditions were rare with northwest surface wind, for which 37% of the P-MPC were coupled. The near surface wind from southwest and southeast is often ~~associated with katabatic flows related with flows from the glaciers~~ (Jocher et al. 2012; Beine et al. 2001; Sect. 3.4) that bring cold air down to the valley in a shallow layer close to the surface. Such a cold surface layer ~~would be~~ is very efficient in decoupling the cloud, ~~and provides an explanation for why the lowest and acts against the cloud driven turbulence that could otherwise couple the P-MPC~~ may be decoupled. ~~The~~ to the surface. This effect might be stronger with southeast than southwest surface wind, since the katabatic winds from southwest are weaker (Fig. 4a). The differences in the coupling of the P-MPC with varying wind conditions can be explained by the differences in stratification of the lower boundary layer under different surface wind conditions. We conclude that the surface wind has the potential to modify the conditions in the boundary layer, which in turn can act to suppress coupling.

The local influence on coupling makes assessing the connection between coupling and cloud properties more challenging. The cloud might have been coupled to the surface while over sea, and when it was advected into ~~Kongsfjorden the Kongsfjorden valley~~ the local wind changed ~~the in~~ the sub-cloud layer ~~which lead leading~~ to decoupling. It is also ~~not possible~~ difficult to evaluate coupling and local winds separately, ~~because most coupled clouds were associated with northwest surface wind (Fig. 13b)~~. Coupled P-MPC had higher LWP than decoupled (Fig. 12a), and P-MPC associated with northwest surface wind had higher LWP than those occurring with other surface wind directions (Fig. ~~10b~~). ~~In fact, most coupled clouds were associated with this surface wind regime (Fig. 11b), and perhaps A1b)~~. Perhaps the higher LWP is related to the combined effect of the two: more humidity is available from the open sea than over land and coupling is required for the water vapor to be transported from the surface to the cloud layer. ~~There is a relationship between surface coupling and the local wind conditions at Ny-Ålesund, but to understand the impact of the combined effects on P-MPC properties would require further studies.~~

5 A consolidated view of P-MPC at Ny-Ålesund

5 Conclusions

655 We presented 2.5 years of vertically resolved cloud observations carried out at the AWIPEV station at Ny-Ålesund. Methods to identify persistent low-level mixed-phase clouds (P-MPC), their coupling to the surface as well as the regional and local wind conditions were developed. We found P-MPC to occur 23 % of the time, most often in summer and least often in winter. The

cloud base was typically 0.54–1.0 km high, LWP 6–52 gm^{-2} , and IWP 0.2–12 gm^{-2} . P-MPC were found to occur at higher altitudes in winter and lower altitudes in summer. LWP presented a lack of seasonal variation, possibly due to the selection of the cloud regime in this study. On the other hand, IWP had a clear seasonal dependence. IWP was low in the relatively warm months of summer and autumn, and had a clear maxima in spring. The frequency of occurrence was found to depend on free-tropospheric wind direction (weather-type), and most P-MPC were associated with westerly winds. The height of the cloud was strongly influenced by orography. ~~Less and higher P-MPC frequent P-MPC and with higher cloud base height~~ were found with easterly winds compared to westerly winds, and these clouds had lower LWP and IWP. The most common surface wind direction in Kongsfjorden ~~was is~~ from southeast, but this ~~was typically underlying is typically underlying synoptic~~ winds from westerly directions. ~~The local wind was found to have an influence on cloud properties in some situations: the LWP was higher for P-MPC with northwest surface wind, and for weather types W and SW the IWP was higher with southeast surface wind. Local winds were not found to impact the occurrence or the height of the P-MPCs, but for some free-tropospheric wind directions the surface wind direction was related to variations in LWP and IWP.~~ P-MPC were mostly decoupled (63–82 % of the time), and coupling occurred most often in summer and for clouds close to the surface. Coupled P-MPC had a higher LWP than decoupled P-MPC, but no differences in IWP were found. Furthermore, the local wind patterns appeared to be related to surface coupling, specifically, the P-MPC with surface wind directions associated with glacier outflows were more commonly decoupled. ~~Some of the observed differences between different wind regimes and coupling states might have been related (e.g. higher LWP were found for coupled P-MPC and for P-MPC associated with northwest surface wind, while coupling was most common for this surface wind direction).~~ The variation of median LWP between different weather types (Fig. 8b) wind direction at 850 hPa was larger than the variation found between different ~~wind regimes (Fig. 10b) surface wind regimes~~ or coupling states (Fig. 12a). On the other hand, ~~for IWP the variation in the medians between weather types (Fig. 8c) was smaller than the differences associated with different wind regimes (Fig. 10c), highlighting the importance of the local influence~~ IWP was found to vary with regional and local wind direction as well as season, but no dependency with coupling to the surface was found. We conclude that while the regional to large scale wind direction was important for P-MPC occurrence and their properties, also the local scale phenomena such as surface coupling and the local flow in the fjord had an influence ~~that cannot be ignored.~~

Our results suggest that the P-MPC water properties can be influenced by the processes in the local boundary layer. The observed LWP values are in the range where the clouds are not yet fully opaque, and changes in LWP will have an impact on the radiative forcing of clouds at Ny-Ålesund (Ebell et al., 2019b) (Ebell et al., 2019a). For numerical models to correctly describe low-level MPC's-MPCs' ice and liquid water content, and hence the radiative effect, the boundary layer dynamics need to be accurately described. In Ny-Ålesund, and in other Arctic fjords, this requires that local wind in the fjord is represented, and thus a description of the orography and key surface properties (temperature, snow cover etc.) needs to be accounted for in the model.

Long-term datasets are valuable for evaluating models since the evaluation can be carried out in a statistical manner instead of case-by-case basis. The dataset presented in this paper can be used for model comparison, to provide insight on model performance regarding low-level MPCs in the complex Arctic fjord environment. In addition, the results presented here provide

background information that aid the interpretation of case studies underway from recent measurement campaigns (Wendisch et al., 2018). In this study, the effects of aerosols acting as ice nucleating particles or cloud condensation nuclei have not been evaluated. Also the cloud micro-physical processes taking place should be considered in more detailed. Further work is thus needed to understand the relationships between various processes controlling the properties and development of low-level MPCs at Ny-Ålesund.

Data availability. The Cloudnet data are available at the Cloudnet website (<http://devcloudnet.fmi.fi/>). The radiosonde data are available in PANGAEA (doi:10.1594/PANGAEA.845373, Maturilli and Kayser (2016) for 1993-2014; doi:10.1594/PANGAEA.875196, Maturilli and Kayser (2017) for 2015-16; search term 'project:label:AC3 ny-alesund radiosonde' afterwards). The meteorological surface observations are available in PANGAEA under search term 'Continuous meteorological observations at station Ny-Ålesund'. The MWR data is also available in PANGAEA (10.1594/PANGAEA.902183, Nomokonova et al. (2019)). The software used for the median test was the courtesy of Keine (2019). The cloud micro-physical dataset is currently under review for PANGAEA (<https://doi.pangaea.de/10.1594/PANGAEA.898556>, Nomokonova and Ebell (2019). Topography data in Fig. 1 are provided by Amante and Eakins (2009) (a) and Norwegian Polar Institute (2014) (b).

Appendix A: [Details on the relationship between local wind conditions and P-MPC](#)

A1 [P-MPC properties](#)

[The results of the analysis on P-MPC properties for different wind regimes is provided here, and some possible mechanism are contemplated.](#) The cloud properties associated with different surface wind directions were compared separately for each weather type. Only weather types N, W and SW were considered ([Fig. A1](#)) in order to have a sufficient amount of data (at least 30 cases) in each group being compared ([Fig. 10 13a](#)). The median liquid base height did not differ significantly (on a 95 % confidence level) for any of the three weather types evaluated. The northwest surface wind was associated with the highest ~~average-median~~ LWP, however, for weather type SW the differences were not statistically significant. For weather type N the median LWP for northwest surface wind was 22 gm^{-2} compared to the the 12 and 7.8 gm^{-2} of southeast and southwest surface winds, [respectively](#). Also for weather type W the northwest surface wind was associated with highest median LWP (39 gm^{-2}), however the lowest median LWP was with southeast surface ~~wine-wind~~ (18 gm^{-2}). The median IWP varied insignificantly (from 7.8 to 9.7 gm^{-2}) for weather type N. For weather type SW, the southwest surface wind had the highest median IWP at 18 gm^{-2} , almost double of the median of southeast (10 gm^{-2}) and northwest (9.1 gm^{-2}) surface winds. Similarly for weather type W the median IWP for southwest was 16 gm^{-2} , and only 11 and 9.6 gm^{-2} for southeast and northwest surface winds. Because of the temperature dependence of many micro-physical processes, it would be possible that the observed differences were a result of different temperature regimes dominating in the compared groups. However, no statistically significant difference in the cloud top temperature distributions ~~were-was~~ found ([Fig. 10d A1d](#)).

Local conditions evidently modify the wind field in the fjord (Sect. 3.4), but whether this affects the P-MPC is not as easily
725 determined. Although we find some differences in the P-MPC occurrence and properties with different local low-level wind
patterns (~~Figures 9 and 10~~[Fig. 13 and A1](#)), these could also be due to the large scale conditions related to different local
circulation patterns. We here consider some phenomena that might be taking place. The near surface wind from southeast
could hinder the low P-MPC residing over the sea from advecting into the fjord where the observations were taking place.
This would lead to higher cloud base height for the southeast surface wind regime, or a lower frequency of occurrence, as the
730 lowest P-MPC would be limited. For both weather types N and W the northwest surface wind had the lowest 25-percentiles
of the liquid layer base height (lower edge of the boxes in ~~Fig. 10a~~[A1a](#)). ~~Fig. 9- 13a~~ gives no indication that the southeast
surface wind would have been related to an overall lower frequency of occurrence. Although the lowest P-MPC were more
often associated with northwest surface wind, liquid base height below 400 m was also not that common for this wind regime.
Hence, it seems that the southeast surface wind was not substantially preventing the P-MPC on the sea from advecting into
735 the fjord. Considering ~~Figures 5 and 10a- 4c and A1a~~ together, the depth of the layer where wind is found to deviate strongest
from the free-tropospheric wind direction is below the median P-MPC base height, and the 25th percentile is above the depth
of the layer where on average the wind is in alignment with the surface wind direction. Hence, many of the P-MPC reside in
a layer where the wind direction is changing with altitude, or just above it. The wind shear could induce turbulence which in
turn could affect the properties of P-MPCs, and it might be influencing vertical fluxes of heat, moisture, and aerosols. These
740 kind of processes could explain the ~~observed differences~~[differences found](#) in IWP and LWP [between different wind regimes](#).
However, to examine these processes would require a more sophisticated description of the local circulation and turbulence in
the boundary layer than was used here.

A2 Seasonality of surface wind direction and P-MPC coupling

Seasonality in near surface wind and the degree of P-MPC coupling with different surface wind directions are presented.
745 Figure A2 shows the windrose for each season for 10 m wind in the studied period, June 2016–October 2018. Differences
between the seasons are present in the relative importance of the three surface wind modes, in agreement with Beine et al. (2001) and
Maturilli and Kayser (2017). The summer months stand out with more common northwesterly winds, which has previously
been attributed to sea breeze (Beine et al., 2001). Subsequently, the other directions are less frequent. In autumn and winter
the northwesterly winds almost completely disappear. The seasonal variation is likely due to the different degree at which
750 the drivers (e.g. sea breeze circulation, katabatic flow, channeling of free-tropospheric wind along the fjord) act in different
seasons.

The relationship between surface wind and P-MPC coupling is similar in all seasons except summer (Fig. A2e-h). In
winter, autumn, and spring coupling with southeast surface wind was rare or non-existent. Coupling mostly occurred with
northwest surface wind. The reasons follow those given in Sect. 4.5: the more (less) stable stratification of the lower boundary
755 layer associated with the southwest (northwest) wind, probably related to the cold outflow from the glaciers that increase the
stability of the sub-cloud layer promoting decoupling. In summer the situation is somewhat different from the other seasons.
Southeast wind was still related to the fewest coupled P-MPC, but the differences between different wind directions were

760 smaller. Furthermore, the coupling frequency with southwest wind was very similar to the northwest wind. The wind roses for each season (Fig. A2a-d) suggest a variation in boundary layer dynamics in summer, which could be contributing to the altered relationship between surface wind direction and the frequency of P-MPC coupling. Moreover, as discussed in Sect. 4.4, the overall lower stability in the boundary layer as well as the lower cloud base height in summer enhance surface coupling compared to the others seasons. Hence, local wind conditions seem to have less importance in summer, although the interaction with the local boundary layer is present in all seasons.

765 *Author contributions.* RG did the method development, statistical analysis, visualization of the results and prepared the manuscript with contributions from all co-authors. UL, SK, and MS contributed with conceptualization, research supervision, and discussions of the results. KE oversaw data management at University of Cologne, and advised in the analysis and selection of data sets. MM provided the long-term radiosonde dataset and insights in the local conditions at Ny-Ålesund.

Competing interests. M. D. Shupe is an editor for the special issue Arctic mixed-phase clouds as studied during the ACLOUD/PASCAL campaigns in the framework of (AC)³.

770 *Acknowledgements.* We gratefully acknowledge the funding by the Deutsche Forschungsgemeinschaft (DFG, German Research Foundation) – Projektnummer 268020496 – TRR 172, within the Transregional Collaborative Research Center “Arctic Amplification: Climate Relevant Atmospheric and SurfaCe Processes, and Feedback Mechanisms (AC)³”. Contributions by Stefan Kneifel were funded by the German Research Foundation (DFG) under grant KN 1112/2-1 as part of the Emmy-Noether Group “Optimal combination of Polarimetric and Triple Frequency radar techniques for Improving Microphysical process understanding of cold clouds (OPTIMIce)”. Contributions by
775 Matthew Shupe were funded by the U.S. National Oceanic and Atmospheric Administration’s Earth System Research Laboratory. We wish to thank the Finnish Meteorological Institute, the Aerosol, Clouds, and Trace Gases Research Infrastructure (ACTRIS), and especially Ewan O’Conner for the Cloudnet algorithm. Furthermore, this work would have not been possible without the contribution of Tobias Marke by his assistance regarding Cloudnet and providing the circulation weather type, as well as Tatiana Nomokonova, who compiled the cloud microphysical dataset and assisted in the use of the MWR data. We further wish to thank Christoph Ritter and Maximilian Mahn for sharing ideas
780 and insightful discussions, and Birte Kulla for providing Fig 1b. Last but not least, we are grateful for the AWIPEV station staff for technical support, maintenance and operation of the instruments.

References

- Amante, C. and Eakins, B.: ETOPO1 1 Arc-Minute Global Relief Model: Procedures, Data Sources and Analysis, NOAA Technical Memo-
785 random NESDIS NGDC-24, <https://doi.org/10.7289/V5C8276M>, 2009.
- Argentini, S., Viola, A. P., Mastrantonio, G., Maurizi, A., Georgiadis, T., and Nardino, M.: Characteristics of the boundary layer at Ny-Ålesund in the Arctic during the ARTIST field experiment, *Annals of Geophysics*, 46, 2003.
- Beine, H., Argentini, S., Maurizi, A., Mastrantonio, G., and Viola, A.: The local wind field at Ny-Ålesund and the Zeppelin mountain at Svalbard, *Meteorol. Atmos. Phys.*, 78, 107–113, 2001.
- 790 Brooks, I. M., Tjernström, M., Persson, P. O. G., Shupe, M. D., Atkinson, R. A., Canut, G., Birch, C. E., Mauritsen, T., Sedlar, J., and Brooks, B. J.: The Turbulent Structure of the Arctic Summer Boundary Layer During The Arctic Summer Cloud-Ocean Study, *J. Geophys. Res.-Atmos.*, 122, 9685–9704, 2017.
- Cesana, G., Kay, J., Chepfer, H., English, J., and De Boer, G.: Ubiquitous low-level liquid-containing Arctic clouds: New observations and climate model constraints from CALIPSO-GOCCP, *Geophys. Res. Lett.*, 39, 2012.
- 795 Chang, L., Song, S., Feng, G., Zhang, Y., and Gao, G.: Assessment of the uncertainties in Arctic low-level temperature inversion characteristics in radio occultation observations, *IEEE T. Geosci. Remote*, 55, 1793–1803, 2017.
- Choi, Y.-S., Ho, C.-H., Park, C.-E., Storelvmo, T., and Tan, I.: Influence of cloud phase composition on climate feedbacks, *J. Geophys. Res.-Atmos.*, 119, 3687–3700, 2014.
- Crewell, S. and Löhnert, U.: Accuracy of Boundary Layer Temperature Profiles Retrieved With Multifrequency Multiangle Microwave
800 Radiometry, *IEEE T. Geosci. Remote*, 45, 2195–2201, <https://doi.org/10.1109/TGRS.2006.888434>, 2007.
- Dahlke, S. and Maturilli, M.: Contribution of Atmospheric Advection to the Amplified Winter Warming in the Arctic North Atlantic Region, *Adv. Meteorol.*, 2017, 2017.
- De Boer, G., Eloranta, E. W., and Shupe, M. D.: Arctic mixed-phase stratiform cloud properties from multiple years of surface-based measurements at two high-latitude locations, *J. Atmos. Sci.*, 66, 2874–2887, 2009.
- 805 Dekhtyareva, A., Holmén, K., Maturilli, M., Hermansen, O., and Graversen, R.: Effect of seasonal mesoscale and microscale meteorological conditions in Ny-Ålesund on results of monitoring of long-range transported pollution, *Polar. Res.*, 37, 1508–1516, 2018.
- Dong, X., Xi, B., Crosby, K., Long, C. N., Stone, R. S., and Shupe, M. D.: A 10 year climatology of Arctic cloud fraction and radiative forcing at Barrow, Alaska, *J. Geophys. Res.-Atmos.*, 115, 2010.
- Ebell, K., Nomokonova, T., Maturilli, M., and Ritter, C.: Radiative effect of clouds at Ny-Ålesund, Svalbard, as inferred from ground-
810 based remote sensing observations, *Journal of Applied Meteorology and Climatology*, <https://doi.org/10.1175/JAMC-D-19-0080.1>, <https://doi.org/10.1175/JAMC-D-19-0080.1>, 2019a.
- Ebell, K., Nomokonova, T., Maturilli, M., and Ritter, C.: Radiative effect of clouds at Ny-Ålesund, Svalbard, as inferred from ground-based remote sensing observations, submitted to *J. Appl. Meteorol. Climatol.*, 2019b.
- Eirund, G. K., Possner, A., and Lohmann, U.: Response of Arctic mixed-phase clouds to aerosol perturbations under different surface
815 forcings, *Atmospheric Chemistry and Physics*, 19, 9847–9864, <https://doi.org/10.5194/acp-19-9847-2019>, <https://www.atmos-chem-phys.net/19/9847/2019/>, 2019.
- Esau, I. and Repina, I.: Wind climate in Kongsfjorden, Svalbard, and attribution of leading wind driving mechanisms through turbulence-resolving simulations, *Adv. Meteorol.*, 2012, 2012.

- Hogan, R. J. and O'Connor, E. J.: Facilitating cloud radar and lidar algorithms: the Cloudnet Instrument Synergy/Target Categorization product, Cloudnet documentation, 2004.
- 820 Hogan, R. J., Jakob, C., and Illingworth, A. J.: Comparison of ECMWF winter-season cloud fraction with radar-derived values, *J. Appl. Meteorol.*, 40, 513–525, 2001.
- Hogan, R. J., Mittermaier, M. P., and Illingworth, A. J.: The retrieval of ice water content from radar reflectivity factor and temperature and its use in evaluating a mesoscale model, *J. Appl. Meteorol. Clim.*, 45, 301–317, 2006.
- 825 Illingworth, A., Hogan, R., O'connor, E., Bouniol, D., Brooks, M., Delanoë, J., Donovan, D., Eastment, J., Gaussiat, N., Goddard, J., et al.: Cloudnet: Continuous evaluation of cloud profiles in seven operational models using ground-based observations, *B. Am. Meteorol. Soc.*, 88, 883–898, 2007.
- Intrieri, J., Fairall, C., Shupe, M., Persson, P., Andreas, E., Guest, P., and Moritz, R.: An annual cycle of Arctic surface cloud forcing at SHEBA, *J. Geophys. Res.-Oceans*, 107, 2002.
- 830 Jackson, R. C., McFarquhar, G. M., Korolev, A. V., Earle, M. E., Liu, P. S., Lawson, R. P., Brooks, S., Wolde, M., Laskin, A., and Freer, M.: The dependence of ice microphysics on aerosol concentration in Arctic mixed-phase stratus clouds during ISDAC and M-PACE, *J. Geophys. Res.-Atmos.*, 117, 2012.
- Jenkinson, A. and Collinson, F.: An initial climatology of gales over the North Sea, *Synoptic climatology branch memorandum*, 62, 18, 1977.
- Jocher, G., Karner, F., Ritter, C., Neuber, R., Dethloff, K., Obleitner, F., Reuder, J., and Foken, T.: The near-surface small-scale spatial and temporal variability of sensible and latent heat exchange in the Svalbard region: a case study, *ISRN Meteorology*, 2012, 2012.
- 835 Kalesse, H., de Boer, G., Solomon, A., Oue, M., Ahlgrimm, M., Zhang, D., Shupe, M. D., Luke, E., and Protat, A.: Understanding Rapid Changes in Phase Partitioning between Cloud Liquid and Ice in Stratiform Mixed-Phase Clouds: An Arctic Case Study, *Mon. Weather Rev.*, 144, 4805–4826, 2016.
- Kay, J. E. and Gettelman, A.: Cloud influence on and response to seasonal Arctic sea ice loss, *J. Geophys. Res.-Atmos.*, 114, 2009.
- 840 Kay, J. E., L'Ecuyer, T., Chepfer, H., Loeb, N., Morrison, A., and Cesana, G.: Recent Advances in Arctic Cloud and Climate Research, *Current Climate Change Reports*, 2, 159–169, 2016.
- Kayser, M., Maturilli, M., Graham, R. M., Hudson, S. R., Rinke, A., Cohen, L., Kim, J.-H., Park, S.-J., Moon, W., and Granskog, M. A.: Vertical thermodynamic structure of the troposphere during the Norwegian young sea ICE expedition (N-ICE2015), *J. Geophys. Res.-Atmos.*, 122, 10–855, 2017.
- 845 Keine, C.: Moods Median Test, <https://www.github.com/ChristianKeine/Moods-Mediantest>, 2019.
- Kim, B.-M., Hong, J.-Y., Jun, S.-Y., Zhang, X., Kwon, H., Kim, S.-J., Kim, J.-H., Kim, S.-W., and Kim, H.-K.: Major cause of unprecedented Arctic warming in January 2016: Critical role of an Atlantic windstorm, *Scientific reports*, 7, 40 051, 2017.
- Klein, S. A., McCoy, R. B., Morrison, H., Ackerman, A. S., Avramov, A., Boer, G. d., Chen, M., Cole, J. N., Del Genio, A. D., Falk, M., et al.: Intercomparison of model simulations of mixed-phase clouds observed during the ARM Mixed-Phase Arctic Cloud Experiment. I: Single-layer cloud, *Q. J. Roy. Meteor. Soc.*, 135, 979–1002, 2009.
- 850 Knudsen, E. M., Heinold, B., Dahlke, S., Bozem, H., Crewell, S., Gorodetskaya, I. V., Heygster, G., Kunkel, D., Maturilli, M., Mech, M., et al.: Meteorological conditions during the ALOUD/PASCAL field campaign near Svalbard in early summer 2017, *Atmos. Chem. Phys.*, 18, 17 995–18 022, 2018.
- Komurcu, M., Storelvmo, T., Tan, I., Lohmann, U., Yun, Y., Penner, J. E., Wang, Y., Liu, X., and Takemura, T.: Intercomparison of the cloud water phase among global climate models, *J. Geophys. Res.-Atmos.*, 119, 3372–3400, 2014.
- 855 Korolev, A. and Isaac, G.: Phase transformation of mixed-phase clouds, *Q. J. Roy. Meteor. Soc.*, 129, 19–38, 2003.

- Küchler, N., Kneifel, S., Löhnert, U., Kollias, P., Czekala, H., and Rose, T.: A W-Band Radar–Radiometer System for Accurate and Continuous Monitoring of Clouds and Precipitation, *J. Atmos. Ocean. Tech.*, 34, 2375–2392, 2017.
- Lamb, D. and Verlinde, J.: *Physics and chemistry of clouds*, Cambridge University Press, 2011.
- 860 Li, Z., Xu, K.-M., and Cheng, A.: The Response of Simulated Arctic Mixed-Phase Stratocumulus to Sea Ice Cover Variability in the Absence of Large-Scale Advection, *J. Geophys. Res.-Atmos.*, 122, 12–335, 2017.
- Löhnert, U. and Crewell, S.: Accuracy of cloud liquid water path from ground-based microwave radiometry 1. Dependency on cloud model statistics, *Radio Sci.*, 38, 2003.
- Maturilli, M. and Ebell, K.: Twenty-five years of cloud base height measurements by ceilometer in Ny-Ålesund, Svalbard, *Earth Syst. Sci. Data*, 10, 1451–1456, 2018.
- 865 Maturilli, M. and Kayser, M.: Homogenized radiosonde record at station Ny-Ålesund, Spitsbergen, 1993-2014, <https://doi.org/10.1594/PANGAEA.845373>, <https://doi.org/10.1594/PANGAEA.845373>, 2016.
- Maturilli, M. and Kayser, M.: Arctic warming, moisture increase and circulation changes observed in the Ny-Ålesund homogenized radiosonde record, *Theor. Appl. Climatol.*, 130, 1–17, 2017.
- 870 Maturilli, M. and Kayser, M.: Homogenized radiosonde record at station Ny-Ålesund, Spitsbergen, 2015-2016, <https://doi.org/10.1594/PANGAEA.875196>, <https://doi.org/10.1594/PANGAEA.875196>, 2017.
- Maturilli, M., Herber, A., and König-Langlo, G.: Climatology and time series of surface meteorology in Ny-Ålesund, Svalbard, *Earth System Science Data*, 5, 155–163, <https://doi.org/10.5194/essd-5-155-2013>, <https://www.earth-syst-sci-data.net/5/155/2013/>, 2013.
- McCoy, D. T., Tan, I., Hartmann, D. L., Zelinka, M. D., and Storelvmo, T.: On the relationships among cloud cover, mixed-phase partitioning, and planetary albedo in GCMs, *J. Adv. Model. Earth Sy.*, 8, 650–668, 2016.
- 875 Mech, M., Kliesch, L.-L., Anhäuser, A., Rose, T., Kollias, P., and Crewell, S.: Microwave Radar/radiometer for Arctic Clouds (MiRAC): first insights from the ALOUD campaign, *Atmospheric Measurement Techniques*, 12, 5019–5037, <https://doi.org/10.5194/amt-12-5019-2019>, <https://www.atmos-meas-tech.net/12/5019/2019/>, 2019a.
- Mech, M., Kliesch, L.-L., Anhäuser, A., Rose, T., Kollias, P., and Crewell, S.: Microwave Radar/radiometer for Arctic Clouds MiRAC: First insights from the ALOUD campaign, *Atmos. Meas. Tech. Disc.*, 2019, 1–32, <https://doi.org/10.5194/amt-2019-151>, 2019b.
- 880 Mioche, G., Jourdan, O., Ceccaldi, M., and Delanoë, J.: Variability of mixed-phase clouds in the Arctic with a focus on the Svalbard region: a study based on spaceborne active remote sensing, *Atmos. Chem. Phys.*, 15, 2445–2461, 2015.
- Mioche, G., Jourdan, O., Delanoë, J., Gourbeyre, C., Febvre, G., Dupuy, R., Monier, M., Szczap, F., Schwarzenboeck, A., and Gayet, J.-F.: Vertical distribution of microphysical properties of Arctic springtime low-level mixed-phase clouds over the Greenland and Norwegian seas, *Atmos. Chem. Phys.*, 17, 12 845–12 869, <https://doi.org/10.5194/acp-17-12845-2017>, 2017.
- 885 Morrison, A., Kay, J., Chepfer, H., Guzman, R., and Yettella, V.: Isolating the liquid cloud response to recent Arctic sea ice variability using spaceborne lidar observations, *J. Geophys. Res.-Atmos.*, 123, 473–490, 2018.
- Morrison, H., Shupe, M. D., Pinto, J. O., and Curry, J. A.: Possible roles of ice nucleation mode and ice nuclei depletion in the extended lifetime of Arctic mixed-phase clouds, *Geophys. Res. Lett.*, 32, 2005.
- 890 Morrison, H., Pinto, J. O., Curry, J. A., and McFarquhar, G. M.: Sensitivity of modeled Arctic mixed-phase stratocumulus to cloud condensation and ice nuclei over regionally varying surface conditions, *J. Geophys. Res.-Atmos.*, 113, 2008.
- Morrison, H., De Boer, G., Feingold, G., Harrington, J., Shupe, M. D., and Sulia, K.: Resilience of persistent Arctic mixed-phase clouds, *Nat. Geosci.*, 5, 11–17, 2012.

- Nomokonova, T. and Ebell, K.: Cloud microphysical properties retrieved from ground-based remote sensing at Ny-Ålesund (10 June 2016 -
895 8 October 2018), <https://doi.org/10.1594/PANGAEA.902183>, <https://doi.pangaea.de/10.1594/PANGAEA.898556>, 2019.
- Nomokonova, T., Ebell, K., Löhnert, U., Maturilli, M., and Ritter, C.: The influence of anomalous atmospheric conditions at Ny-Ålesund
on clouds and their radiative effect, *Atmospheric Chemistry and Physics Discussions*, 2019, 1–34, <https://doi.org/10.5194/acp-2019-985>,
<https://www.atmos-chem-phys-discuss.net/acp-2019-985/>, 2019a.
- Nomokonova, T., Ebell, K., Löhnert, U., Maturilli, M., Ritter, C., and O'Connor, E.: Statistics on clouds and their relation to thermodynamic
900 conditions at Ny-Ålesund using ground-based sensor synergy, *Atmos. Chem. Phys.*, 19, 4105–4126, [https://doi.org/10.5194/acp-19-4105-](https://doi.org/10.5194/acp-19-4105-2019)
2019, <https://www.atmos-chem-phys.net/19/4105/2019/>, 2019b.
- Nomokonova, T., Ritter, C., and Ebell, K.: HATPRO microwave radiometer measurements at AWIPEV, Ny-Ålesund (2016–2018),
<https://doi.org/10.1594/PANGAEA.902183>, <https://doi.pangaea.de/10.1594/PANGAEA.902183>, 2019.
- Norgren, M. S., Boer, G. d., and Shupe, M. D.: Observed aerosol suppression of cloud ice in low-level Arctic mixed-phase clouds, *Atmos.*
905 *Chem. Phys.*, 18, 13 345–13 361, 2018.
- Norwegian Polar Institute: Kartdata Svalbard 1:100 000 (S100 Kartdata) /Map Data [Data set],
<https://doi.org/10.21334/npolar.2014.645336c7>, 2014.
- Pithan, F., Svensson, G., Caballero, R., Chechin, D., Cronin, T. W., Ekman, A. M., Neggers, R., Shupe, M. D., Solomon, A., Tjernström, M.,
et al.: Role of air-mass transformations in exchange between the Arctic and mid-latitudes, *Nat. Geosci.*, 11, 805, 2018.
- 910 Qiu, S., Xi, B., and Dong, X.: Influence of Wind Direction on Thermodynamic Properties and Arctic Mixed-Phase Clouds in Autumn at
Utqiagvik, Alaska, *J. Geophys. Res.-Atmos.*, 123, 9589–9603, 2018.
- Quinn, P., Shaw, G., Andrews, E., Dutton, E., Ruoho-Airola, T., and Gong, S.: Arctic haze: current trends and knowledge gaps, *Tellus B:*
Chemical and Physical Meteorology, 59, 99–114, 2007.
- Rose, T., Crewell, S., Löhnert, U., and Simmer, C.: A network suitable microwave radiometer for operational monitoring of the cloudy
915 atmosphere, *Atmos. Res.*, 75, 183–200, 2005.
- Savre, J., Ekman, A. M., Svensson, G., and Tjernström, M.: Large-eddy simulations of an Arctic mixed-phase stratiform cloud observed
during ISDAC: sensitivity to moisture aloft, surface fluxes and large-scale forcing, *Q. J. Roy. Meteor. Soc.*, 141, 1177–1190, 2015.
- Scott, R. C. and Lubin, D.: Unique manifestations of mixed-phase cloud microphysics over Ross Island and the Ross Ice Shelf, Antarctica,
Geophys. Res. Lett., 43, 2936–2945, 2016.
- 920 Sedlar, J., Shupe, M. D., and Tjernström, M.: On the relationship between thermodynamic structure and cloud top, and its climate significance
in the Arctic, *J. Climate*, 25, 2374–2393, 2012.
- Serreze, M., Barrett, A., Stroeve, J., Kindig, D., and Holland, M.: The emergence of surface-based Arctic amplification, *The Cryosphere*, 3,
11, 2009.
- Serreze, M. C. and Barry, R. G.: Processes and impacts of Arctic amplification: A research synthesis, *Global Planet. Change*, 77, 85–96,
925 2011.
- Sheskin, D.: *Handbook of Parametric and Nonparametric Statistical Procedures*, CRC Press, 2 edn., 2000.
- Shupe, M. D.: Clouds at Arctic atmospheric observatories. Part II: Thermodynamic phase characteristics, *J. Appl. Meteorol. Clim.*, 50, 645–
661, 2011.
- Shupe, M. D. and Intrieri, J. M.: Cloud radiative forcing of the Arctic surface: The influence of cloud properties, surface albedo, and solar
930 zenith angle, *J. Climate*, 17, 616–628, 2004.

- Shupe, M. D., Kollias, P., Matrosov, S. Y., and Schneider, T. L.: Deriving mixed-phase cloud properties from Doppler radar spectra, *J. Atmos. Ocean. Tech.*, 21, 660–670, 2004.
- Shupe, M. D., Matrosov, S. Y., and Uttal, T.: Arctic mixed-phase cloud properties derived from surface-based sensors at SHEBA, *J. Atmos. Sci.*, 63, 697–711, 2006.
- 935 Shupe, M. D., Kollias, P., Persson, P. O. G., and McFarquhar, G. M.: Vertical motions in Arctic mixed-phase stratiform clouds, *J. Atmos. Sci.*, 65, 1304–1322, 2008.
- Shupe, M. D., Walden, V. P., Eloranta, E., Uttal, T., Campbell, J. R., Starkweather, S. M., and Shiobara, M.: Clouds at Arctic atmospheric observatories. Part I: Occurrence and macrophysical properties, *J. Appl. Meteorol. Clim.*, 50, 626–644, 2011.
- Shupe, M. D., Persson, P. O. G., Brooks, I. M., Tjernström, M., Sedlar, J., Mauritsen, T., Sjogren, S., and Leck, C.: Cloud and boundary layer
940 interactions over the Arctic sea ice in late summer, *Atmos. Chem. Phys.*, 13, 9379–9399, <https://doi.org/10.5194/acp-13-9379-2013>, 2013.
- Solomon, A., Shupe, M. D., Persson, O., Morrison, H., Yamaguchi, T., Caldwell, P. M., and de Boer, G.: The sensitivity of springtime Arctic mixed-phase stratocumulus clouds to surface-layer and cloud-top inversion-layer moisture sources, *J. Atmos. Sci.*, 71, 574–595, 2014.
- Solomon, A., de Boer, G., Creamean, J. M., McComiskey, A., Shupe, M. D., Maahn, M., and Cox, C.: The relative impact of cloud condensation nuclei and ice nucleating particle concentrations on phase partitioning in Arctic mixed-phase stratocumulus clouds, *Atmos. Chem. Phys.*, 18, 17 047–17 059, <https://doi.org/10.5194/acp-18-17047-2018>, 2018.
- 945 Solomon, S., Qin, D., Manning, M., Averyt, K., and Marquis, M.: *Climate change 2007-the physical science basis: Working group I contribution to the fourth assessment report of the IPCC, vol. 4*, Cambridge university press, 2007.
- Sotiropoulou, G., Sedlar, J., Tjernström, M., Shupe, M. D., Brooks, I. M., and Persson, P. O. G.: The thermodynamic structure of summer Arctic stratocumulus and the dynamic coupling to the surface, *Atmos. Chem. Phys.*, 14, 12 573–12 592, 2014.
- 950 Svendsen, H., Beszczynska-Møller, A., Hagen, J. O., Lefauconnier, B., Tverberg, V., Gerland, S., Børre Ørbæk, J., Bischof, K., Papucci, C., Zajaczkowski, M., et al.: The physical environment of Kongsfjorden–Krossfjorden, an Arctic fjord system in Svalbard, *Polar research*, 21, 133–166, 2002.
- Wendisch, M., Macke, A., Ehrlich, A., Lüpkes, C., Mech, M., Chechin, D., Dethloff, K., Barrientos, C., Bozem, H., Brückner, M., et al.: The Arctic Cloud Puzzle: Using ALOUD/PASCAL Multi-Platform Observations to Unravel the Role of Clouds and Aerosol Particles in
955 Arctic Amplification, *B. Am. Meteorol. Soc.*, 2018.
- Wendish et al.: *Understanding Causes and Effects of Rapid Warming in the Arctic*, 2017.
- Westbrook, C. D. and Illingworth, A. J.: Evidence that ice forms primarily in supercooled liquid clouds at temperatures > -27 C, *Geophys. Res. Lett.*, 38, 2011.
- Woods, C., Caballero, R., and Svensson, G.: Large-scale circulation associated with moisture intrusions into the Arctic during winter, *Geophys. Res. Lett.*, 40, 4717–4721, 2013.
- 960 Yamartino, R. J.: A comparison of several “single-pass” estimators of the standard deviation of wind direction, *J. Clim. Appl. Meteorol.*, 23, 1362–1366, 1984.
- Young, G., M Jones, H., Choulaton, T., Crosier, J., Bower, K. N., Gallagher, M. W., Davies, R. S., Renfrew, I., Elvidge, A., Darbyshire, E., et al.: Observed microphysical changes in Arctic mixed-phase clouds when transitioning from sea ice to open ocean, *Atmos. Chem. Phys.*,
965 16, 13 945–13 967, 2016.
- Zängl, G., Reinert, D., Rípodas, P., and Baldauf, M.: The ICON (ICOsahedral Non-hydrostatic) modelling framework of DWD and MPI-M: Description of the non-hydrostatic dynamical core, *Q. J. Roy. Meteor. Soc.*, 141, 563–579, 2015.

- Zhao, M. and Wang, Z.: Comparison of Arctic clouds between European Center for Medium-Range Weather Forecasts simulations and Atmospheric Radiation Measurement Climate Research Facility long-term observations at the North Slope of Alaska Barrow site, *J. Geophys. Res.-Atmos.*, 115, 2010.
- 970
- Zuidema, P., Baker, B., Han, Y., Intrieri, J., Key, J., Lawson, P., Matrosov, S., Shupe, M., Stone, R., and Uttal, T.: An Arctic springtime mixed-phase cloudy boundary layer observed during SHEBA, *J. Atmos. Sci.*, 62, 160–176, 2005.

Table 1. The instruments used, the most relevant specifications of each measurement, together with an overview of derived parameters. If the vertical (Δz) or temporal resolution (Δt) is changed from that measured by the instrument, the resolution used in the analysis is given in the last column.

	Instrument	Temporal resolution	Vertical resolution	Parameters measured	Derived parameters
JOYRAD-94	RPG-FMWC94-SP	2-3 sec	100-400 m: 4 m 400-1200 m: 5.3 m	Radar reflectivity (Z_e), Doppler velocity (V_m)	Cloud presence, cloud boundaries (by Cloudnet; $\Delta z = 20$ m, $\Delta t = 30$ s)
		2-3 sec	1.2-3 km: 6.7 m		
MIRAC-A		2-3 sec	100-400 m: 3.2 m 400-1200 m: 7.5 m 1.2-3 km: 9.7 m		Ice water content (IWC) $\Delta z = 20$ m, $\Delta t = 30$ s
Microwave radiometer	HATPRO	1 sec	-	Brightness temperatures at 22.24-31.40 GHz	Liquid water path (LWP)
		15-20 min	-	Brightness temperatures at 51.26-58 GHz	Potential temperature (θ) -profiles, $\Delta z = 50$ -250 m in the lowest 2.5 km
Ceilometer	Vaisala CL51	12-20 s	10 m	Attenuated backscatter (β) at 905 nm	Cloud base, liquid presence (by Cloudnet; $\Delta z = 20$ m, $\Delta t = 30$ s)
	Thies Clima PT100		Measurement at 2 and 10 m	Temperature	Potential temperature (θ)
Surface meteorology	Paroscientific, Inc. 6000-16B	1 min	-	Pressure	
	Combined Wind Sensor Classic, Thies Clima		Measurement at 10 m	Wind speed and direction	30 min mean wind speed and direction
Radiosonde	RS92, RS41	At least 1/day	5-7 m	Temperature, Pressure	Potential temperature (θ)
				Wind direction	Wind direction

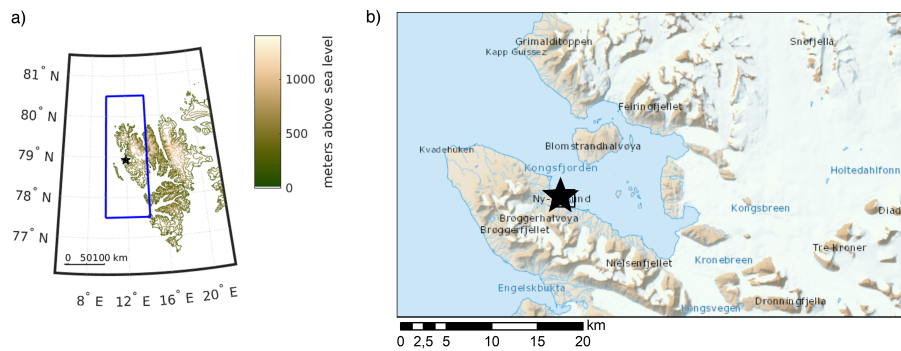


Figure 1. Topography map for Svalbard (a) and [a detailed illustration of](#) the Kongsfjorden area (b). The black star indicates the location of Ny-Ålesund, where the measurements are taken. The domain covered by the circulation weather type (~~CWT~~, see Sect. 3.3) is shown by the blue rectangle. Topography data by Amante and Eakins (2009) (a) and [the](#) Norwegian Polar Institute (2014) (b).

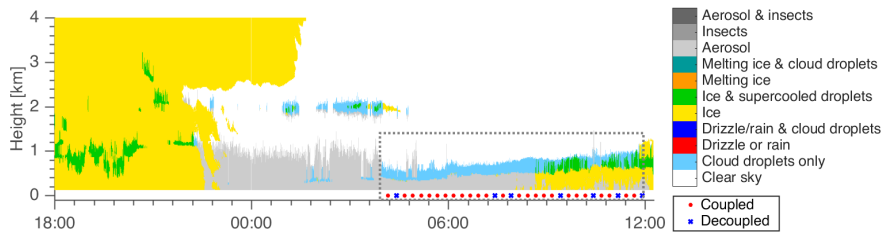


Figure 2. Example of the Cloudnet target classification product ~~for 29–30~~ from 29 May 2018, 18 UTC to 30 May 2018, 12 UTC. For the P-MPC, indicated by the gray dashed box, also the time series of coupling is shown. This case was classified as coupled.

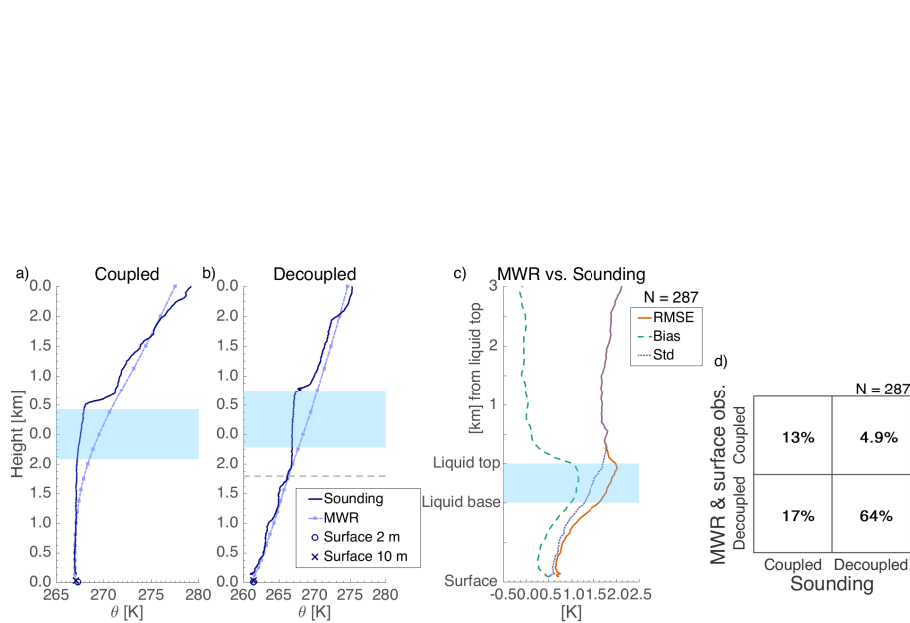


Figure 3. Examples of θ -profiles from sounding and MWR, as well as surface observations: a coupled cloud on the 24 October 2017 11:55–12:05 UTC (a) and a decoupled cloud on the 1 February 2018 16:47–16:56 (b). The blue shaded area indicates the cloud layer, where cloud base and top are determined as the median values of the Cloudnet based cloud base and top for the duration of the sounding. The gray dashed line indicates the decoupling height defined from the sounding θ -profile. Comparison of potential temperature profiles from sounding and retrieved from MWR measurements ~~-all data (a) and only~~ when P-MPC were present, with height normalized in respect to the liquid layer (bc). Comparison of the diagnosed coupling with the new method based on MWR and surface observations and based on sounding profiles (ed).

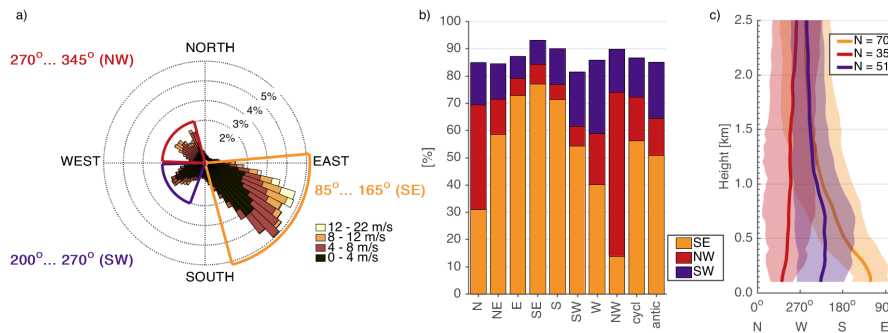


Figure 4. Wind rose for 30 min mean 10 m wind for the cloud observation period (June 2016–October 2018) with the three main modes identified (a), and the relative frequency of occurrence for each weather type (b). Wind direction distribution profiles corresponding to each identified near surface wind direction mode for weather type W (a) and N (b) based on radiosoundings from August 2011–June 2016 to October 2018–2018 (c). The line shows the mean wind direction, and the shaded area the mean \pm standard deviation at each height, estimated using the method by Yamartino (1984). All data points with wind speed below 0.5 ms^{-1} were omitted. N gives the number of soundings available for each mean profile.

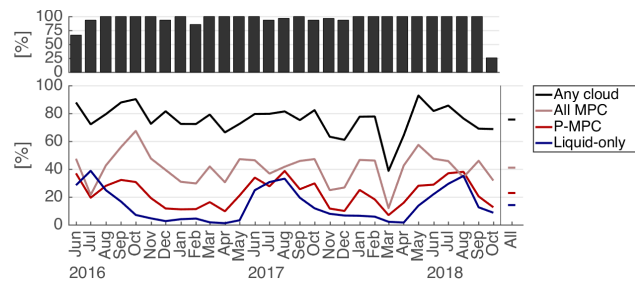


Figure 5. Monthly and total occurrence frequency of clouds in general and selected specific cloud types (see text for definitions) on bottom, coverage of Cloudnet data on top.

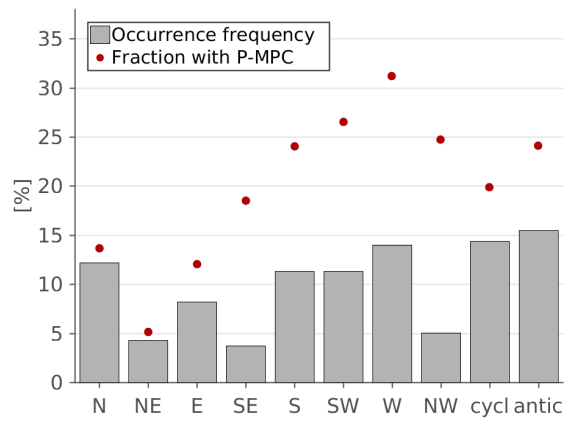


Figure 6. The frequency of occurrence of each weather type and the fraction with P-MPC presence.

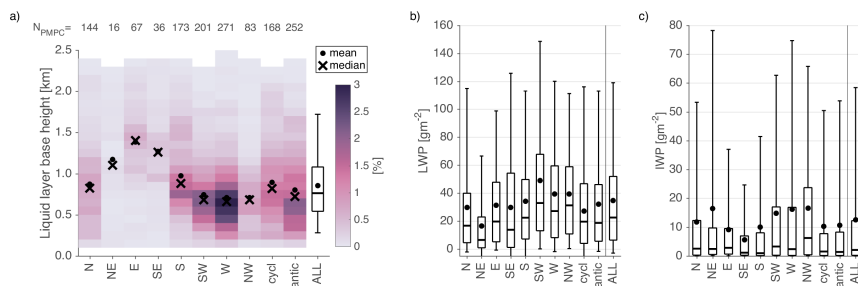


Figure 7. Height of the P-MPC liquid layer base (a), the LWP (b) and IWP (c) distributions for each weather type and all P-MPC. The number of P-MPC cases for each weather type is given in (a). The box shows the 25th, 50th and 75th percentile, the dot the mean, and the whiskers indicate the 5th and 95th percentile. The medians for different weather types were found to differ on a 95 % confident level.

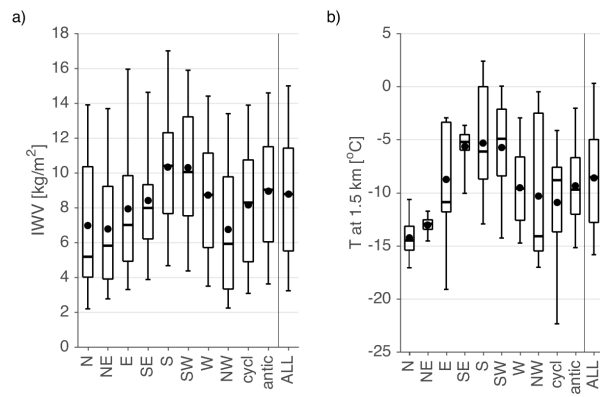


Figure 8. IWV (a) and 1.5 km temperature (b) for time periods with P-MPC present for each weather type. Boxes and whiskers as in Fig. 7. The medians were found to differ on a 95 % confidence level.

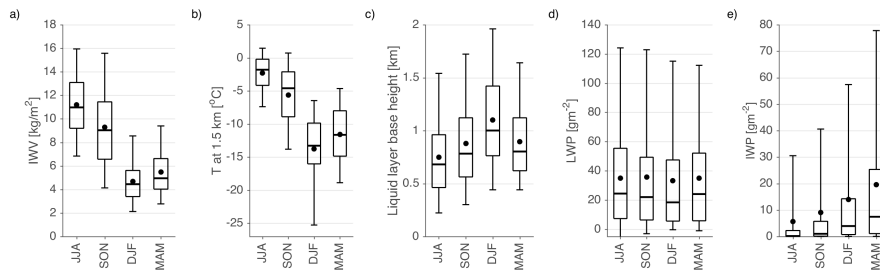


Figure 9. IWV (a), 1.5 km temperature (b), liquid base height (c), LWP (d) and IWP (e) distributions for each season. Only time periods with P-MPCs present are included. Boxes and whiskers as in Fig. 7; the medians were found to differ on a 95 % confident level.

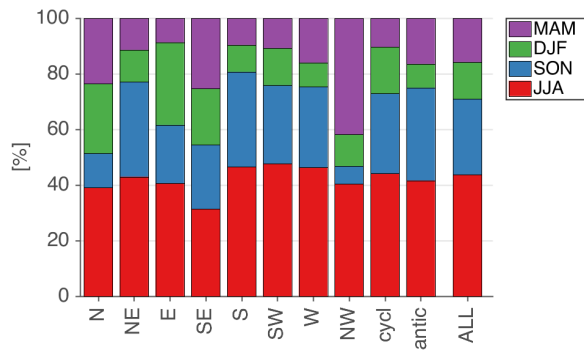


Figure 10. Distribution of seasons in the studied data set for each weather type. Only time periods when a P-MPC was present are included to evaluate the possible impact of wind direction seasonality on cloud properties and occurrence.

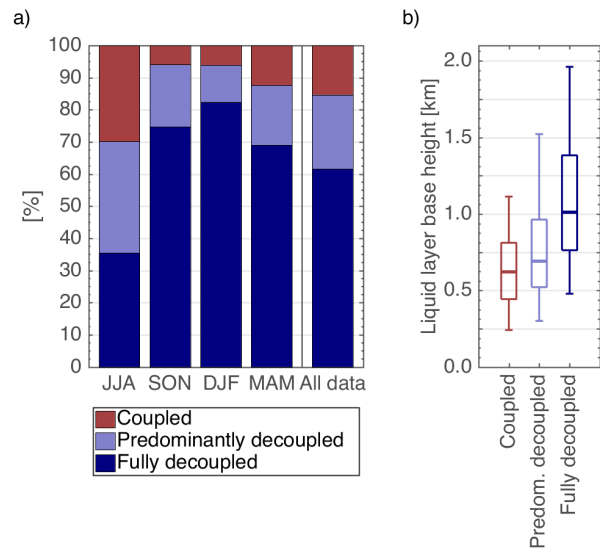


Figure 11. The fraction of P-MPC cases classified as coupled, predominantly decoupled and fully decoupled in each season and for the entire data set (a), for each surface wind direction regime (b) as well as and the distribution of the liquid layer base height in the coupling classes as well as for each season (c). The liquid base height distributions for each season in (c) include all P-MPC independent of coupling state. Boxes and whiskers as in Fig. 7; the medians were found to differ on a 95 % confident level between coupling classes and between seasons.

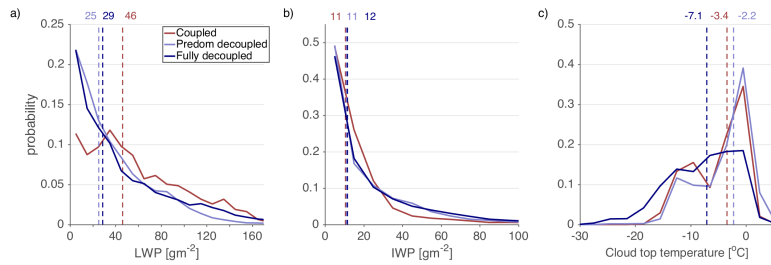


Figure 12. Comparison of LWP (a), IWP (b), and cloud top temperature (c) distributions between P-MPC in weather types W and SE with different degree of surface coupling. The dashed line and the numbers on top show the median value of each distribution. The bin size for LWP and IWP is 10 gm^{-2} and for cloud top temperature 3°C . For all parameters the The medians were found to differ on a 95 % confident level for LWP and cloud top temperature.

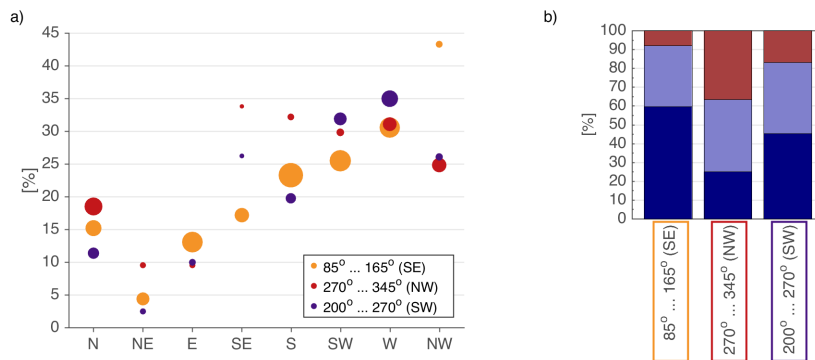


Figure 13. Fraction of time with P-MPC occurring for each surface wind direction and weather type regime (a). The size of the dot represents the amount of data available to compute the value. The fraction of P-MPC cases classified as coupled, predominantly decoupled and fully decoupled for each surface wind direction mode (b).

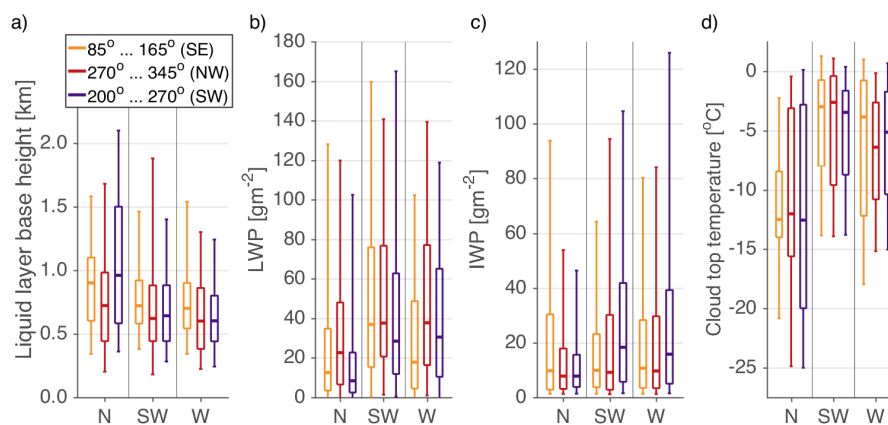


Figure A1. P-MPC liquid layer base height (a), LWP (b), IWP (c), and cloud top temperature (d) distributions for selected weather types and surface wind directions. Boxes and whiskers as in Fig. 7. The medians were found to differ (on a 95 % confidence level) in LWP for N and W, and IWP for SW and W.

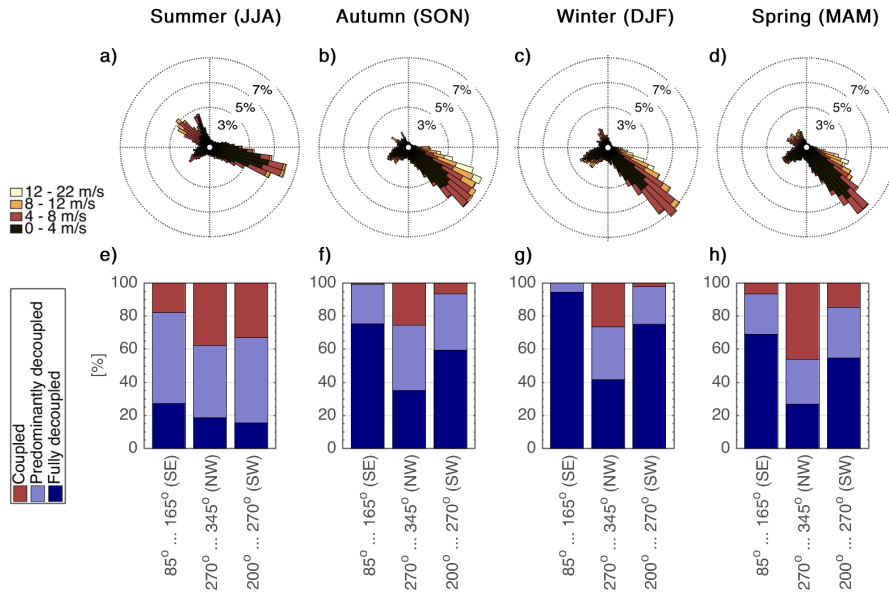


Figure A2. Wind rose for 30 min mean 10 m wind for each season (a-d) in the cloud observation period (June 2016–October 2018). The fraction of P-MPC cases classified as coupled, predominantly decoupled and fully decoupled for each surface wind direction mode in each season (e-f).